Australian Journal of Earth Sciences
An International Geoscience Journal of the Geological Society of Australia

ISSN: 0812-0099 (Print) 1440-0952 (Online) Journal homepage: www.tandfonline.com/journals/taje20

An overview of gold systems in Uganda

C. Nyakecho & S. G. Hagemann

To cite this article: C. Nyakecho & S. G. Hagemann (2014) An overview of gold systems in Uganda, Australian Journal of Earth Sciences, 61:1, 59-88, DOI: 10.1080/08120099.2013.831773

To link to this article: https://doi.org/10.1080/08120099.2013.831773

Australian Journal of Earth Sciences (2014)
61, 59–88, http://dx.doi.org/10.1080/08120099.2013.831773

An overview of gold systems in Uganda

C. NYAKECHO* **and S. G. HAGEMANN**

University of Western Australia, School of Earth and Sciences, Centre for Exploration Targeting,
35 Stirling Highway, Crawley, WA 6009, Australia.

Detailed analyses of historic and recent information on active and abandoned gold mines and alluvial workings in combination with new regional geochronology, documentation and interpretation of the lithostratigraphy, structural setting, hydrothermal alteration and mineralisation, and geochemistry of mineralised rocks have formed the basis for the definition of four major gold districts in Uganda: (1) the Busia gold district hosted in the Neoarchean Busia-Kakamega granite–greenstone belt in the SE of Uganda, which contains the structurally controlled mesozonal Tira gold mine; (2) the Mubende gold district in the Paleoproterozoic Rwenzori fold belt in central Uganda, which hosts the structurally controlled metasediment-hosted mesozonal Kamalenge and Kisita gold mines; (3) the Buhweju-Mashonga gold district in SW Uganda, which contains the vein hosted Pb–Zn–Au Kitaka mine, the structurally controlled intrusion-hosted mesozonal Mashonga gold mine and the structurally controlled sandstone-hosted mesozonal Muti and Kanywambogo mines; and (4) the Karamoja gold district, which is hosted in reworked Archean basement rocks and/or in the upper amphibolite–lower granulite facies rocks of the Neoproterozoic Mozambique fold belt in NE and W Uganda and in the northern part of the Karamoja gold district containing numerous hypozonal shear zone-controlled gold workings. Other areas in Uganda where alluvial gold mineralisation and/or shallow gold workings are reported comprise the Kitgum area within the Aswa shear zone in northern Uganda, the Western Nile area, which represents the western extremity of the Bomu-Kibalian shield of NE Congo, and the Kabale-Kisoro area hosted in the Mesoproterozoic North Kibaran fold belt in SW Uganda. The results of this work are an early attempt to portray the gold metallogeny of Uganda. Future studies, including geological mapping at all scales, geochronology, whole-rock geochemistry and chemical and mineralogical studies of mineralised samples, will help clarify the distribution and origin of diverse gold systems in this poorly understood part of Africa.

KEYWORDS: Uganda, gold, orogenic gold, mining, exploration, structural controls, hydrothermal alteration.

INTRODUCTION

Uganda is located in East Africa and is bordered by Kenya in the east, Tanzania and Rwanda in the south, Democratic Republic of Congo (DRC) in the west and South Sudan in the north. Geologically, Uganda is located within the African Plate, which consists of several accreted Archean cratons (e.g. Uganda, Tanzania and Congo cratons) that have been welded together by Proterozoic mobile belts such as the Ubendian, Usagaran and Kibaran belts (Begg *et al.* 2009). This accretionary setting represents a favourable geodynamic setting for orogenic and intrusion-related gold mineralisation (e.g. Kerrich *et al.* 2000; Groves *et al.* 2003, 2005; Goldfarb *et al.* 2005). Despite the favourable geodynamic setting for gold in much of Uganda, including the Archean granite–greenstone belts in the SW and NW of Uganda, and the Paleoproterozoic metasedimentary mobile belts in central and SW Uganda, and the existence of some gold mines, there is a dearth of world-class gold deposits. The lack of exploitation and exploration for gold is partly explained by the absence of modern geological maps and descriptions of the tectonic setting, including structural analyses of many terranes in Uganda, and the near complete lack of documentation of existing gold mines with respect to the lithostratigraphy, structure and hydrothermal alteration and mineralisation.

One factor contributing to the lack of exploration and mining investment in Uganda was caused by the difficult economic situation from the mid 1970s to the end of the 1980s, but in the 1980s the Ugandan government introduced mining laws and regulations and financed several small projects but hampered by a lack of regional geological mapping, and regional geophysical and geochemical surveys of the geologically diverse regions. In 2004, the government of Uganda obtained funding from the World Bank, the Nordic Development Bank and the African Development Bank, and initiated the ‘Sustainable Management of Mineral Resources Project (SMMRP).’ The goal was to acquire extensive geoscientific data and develop information on mineral resources. This project was conducted between 2004 and 2012 by Fugro and the Geological Survey of Finland (GTK) in partnership with the Geological Survey of Uganda and other agencies.

---

*Corresponding author: ncathy.geology@gmail.com

This research project was initiated by the Geological Survey of Uganda and the Centre for Exploration Targeting in order to define significant gold districts based on the evaluation of historic and recently acquired data sets (e.g. geochronology), combined with observations in the field and new petrographic and geochemical data.

This paper is organised in three parts: first the timing and tectonic setting of the geological units in Uganda are presented in order to provide a coherent geological framework based on the geological setting of the gold districts. This is followed by the geological description of four major gold districts, including abandoned and presently producing mine sites, and other areas where, for example, alluvial gold workings and/or significant Au values from soil or rock chip samples are known. The last part provides a discussion about gold systems in Uganda and suggestions for future work.

TIMING AND TECTONIC SETTING OF THE GEOLOGICAL UNITS IN UGANDA

The tectonic events in Uganda span over three billion years of geological history (Schlüter & Hampton 1997), starting with the formation of Mesoarchean cratonic crust and closing with the development of the Albertine Rift, filled by a Neogene succession of alkaline volcanic products, associated carbonatites and subordinate terrestrial sediments, mostly covered by Holocene alluvial deposits (Figure 1). Most gold occurrences are hosted in Archean granite–greenstone belts and Proterozoic mobile belts.

The Archean in Uganda

According to Westerhof (2012) and Begg *et al.* (2009), the Archean rocks in Uganda have been divided into four terranes (Figure 2): (1) West Nile Terrane, (2) Northern Uganda Terrane, (3) West Tanzania Terrane and (4) Lake Victoria Terrane. The West Nile Terrane is the eastern segment of the Bomu-Kibalian shield of NE Congo, which has been described as the ‘Formation du Nil occidental’ (West Nile Gneiss Formation) or Garamba Gneiss Complex (Cahen & Snelling 1984). It consists of NNE-trending belts of tonalitic to monzogranitic granitoids and gneisses, and Neoarchean sedimentary cover, dated at 2.9–2.6 Ga using U/Pb geochronology on zircons (Mänttäri 2011).

The North Uganda Terrane is composed of a complex assembly of Neoarchean (2.66–2.63 Ga using U/Pb geochronology on zircons; Mänttäri 2011) mildly deformed granitoids and moderately to strongly deformed gneisses and migmatites; however, granodiorites and tonalites are predominant. The North Uganda Terrane and West Nile Terrane contain, in addition, Mesoarchean granulites and charnockites dated at 2.99 Ga and >3.08 Ga (U/Pb geochronology on zircon cores; Mänttäri 2011), respectively (De Kock *et al.* 2012).

The West Tanzania Terrane (2.65–2.64 Ga with 2.8 Ga U/Pb geochronology on zircon cores; Baglow *et al.* 2012a)

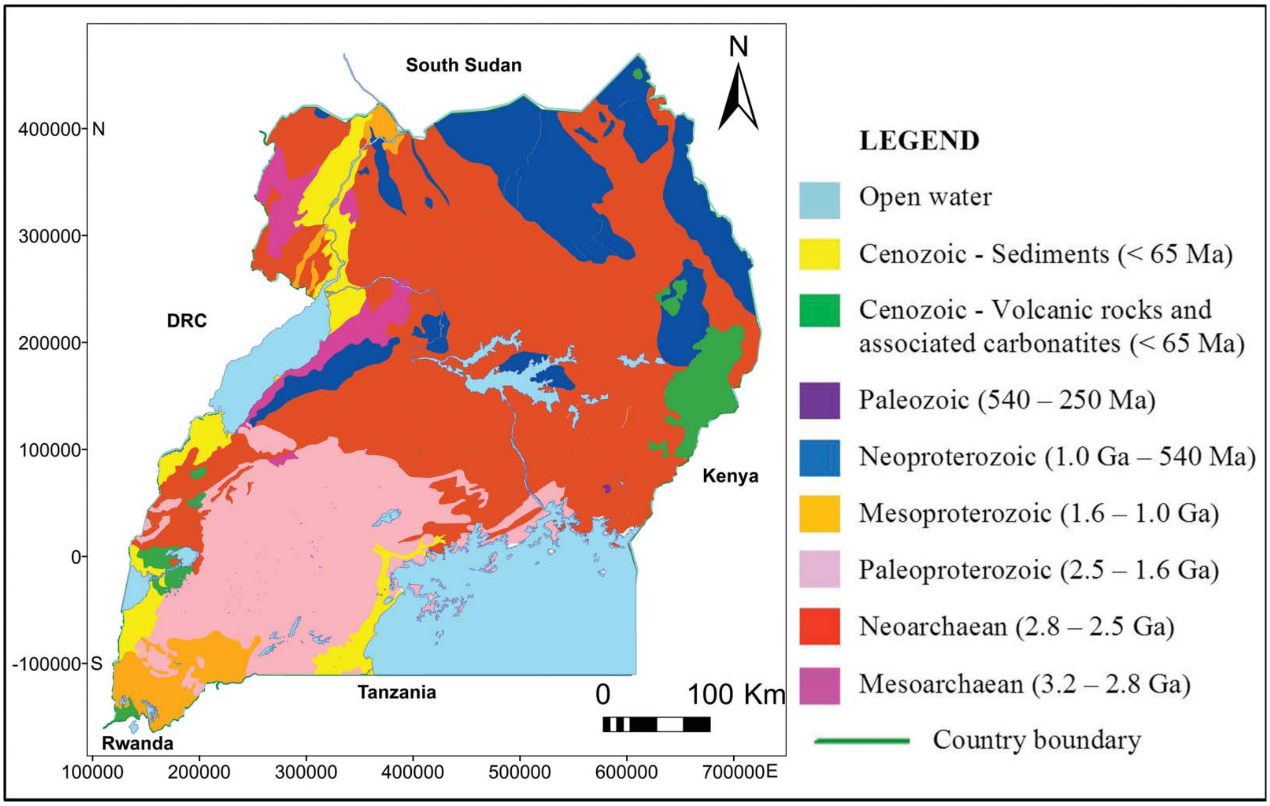

Figure 1 The geological eras of Uganda constructed by using available geochronological datasets of Uganda including Hepworth & Macdonald (1966), Schlüter & Hampton (1997), Begg *et al.* (2009), Elepu *et al.* (2010a, 2011a), Mänttäri (2010a, b, 2011), Baglow *et al.* (2011, 2012a, b), and De Kock *et al.* (2012).

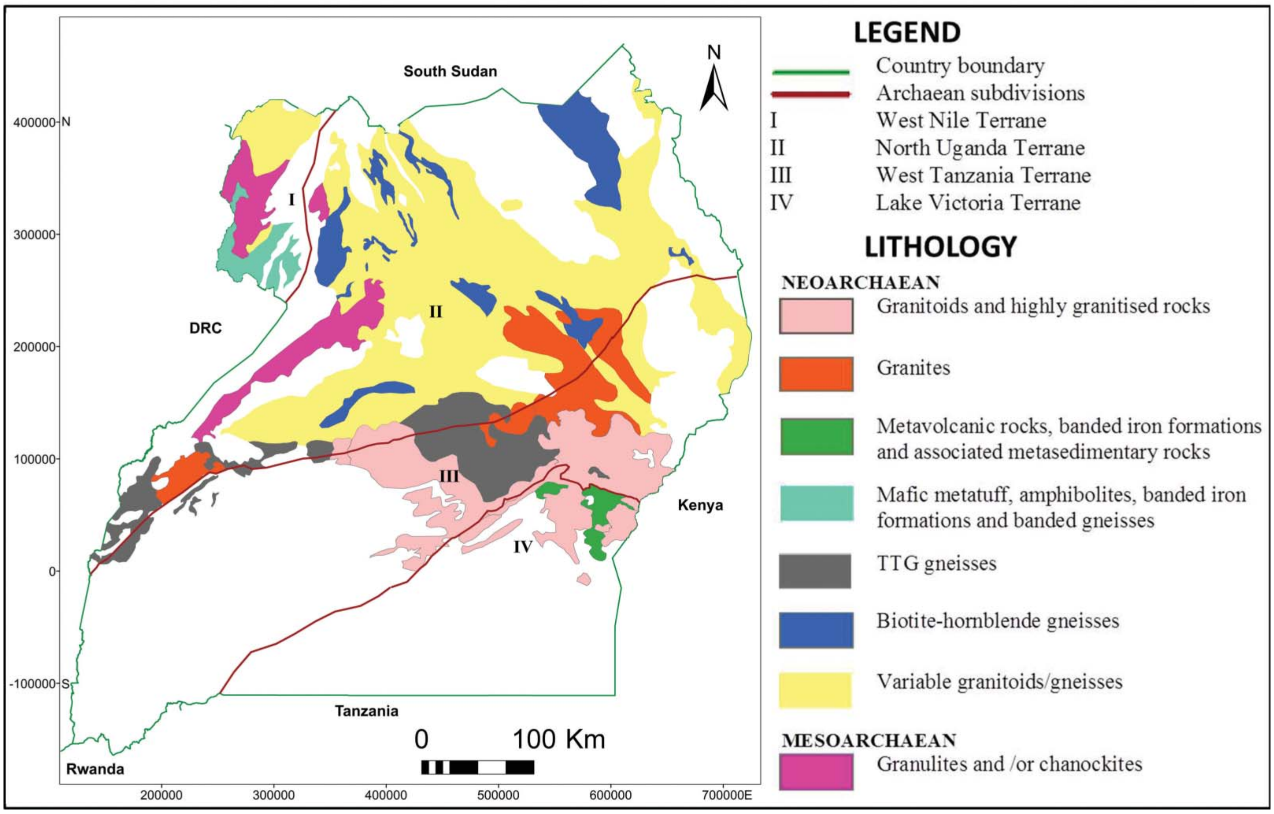

Figure 2 Geological map of Uganda displaying the Archean terranes and lithologies. The map was constructed using available geochronological datasets of Uganda including Hepworth & Macdonald (1966), Schlüter & Hampton (1997), Begg *et al.* (2009), Elepu *et al.* (2011a), Mänttäri (2010a, b, 2011), Baglow *et al.* (2011, 2012a, b), and De Kock *et al.* (2012).

belongs to the Tanzania Craton and consists of granite–gneiss–migmatite, mostly exposed S of Lake Kyoga and also continuing into Tanzania where it occupies the western segment of the Tanzania Craton (Baglow *et al.* 2012a). The Tanzania Craton of East Africa consists of 2.8–2.5 Ga granitoids, which intruded many large and small greenstone belts (Borg & Shackleton 1997). Peak metamorphic conditions, which ranged from greenschist to granulite facies, were characterised by abundant emplacement of syn- and post-metamorphic intrusions, clustering around 1.8 Ga (Borg & Shackleton 1997).

The Lake Victoria Terrane represents a classic Neoarchean (2.64–2.59 Ga) granite–greenstone terrane, belonging to the Tanzania Craton and is restricted to the SE of Uganda, next to the Kenyan border (Baglow *et al.* 2012a). The Lake Victoria Terrane was termed the Busia-Kakamega greenstone belt (Gabert 1990). The Lake Victoria Terrane in northern Tanzania is known for its world-class orogenic gold deposits in the Archean greenstone belt, e.g. in the Musoma, Iramba-Sekenke and Southwest Mwanza goldfields. The Busia-Kakamega greenstone belt consists of metavolcanic rocks, banded iron formations (BIF) and associated low-grade metasedimentary rocks of the Nyanzian Supergroup (Hester 2009). Alkaline bodies, and a cluster of gabbroic pipes, intruded the Archean Lake Victoria granite–gneiss terrane (Elepu *et al.* 2011a). Supracrustal rocks are derived from Archean (2.6 Ga) granitoids and the Kavirondian Supergroup. The latter, according to Cahen & Snelling (1984), has a minimum whole-rock Rb–Sr isochron age of 2.4 Ga and a maximum whole-rock Rb–Sr isochron age of 2.7 Ga.

The Proterozoic in Uganda

There are at least three major Proterozoic belts exposed in Uganda; the Paleoproterozoic Rwenzori fold belt, the Mesoproterozoic North Kibaran belt and the Neoproterozoic Mozambique belt (Figure 3).

The Paleoproterozoic Rwenzori fold belt (2.1–1.85 Ga) constitutes the Ugandan segment of a system of fold belts wrapping around the Tanzania Craton. The rocks comprise a cover sequence of the Buganda metavolcano-sedimentary rocks estimated at 2.0 Ga (Baglow *et al.* 2011), deposited on Archean and Paleoproterozoic basement gneiss with a U/Pb on zircon age of 2147 ± 16 Ma (Mänttäri 2010a). These rocks were intruded by two generations of granitoids (Figure 4). The oldest granitoids are attributed to the Sembubule Suite with a U/Pb zircon age of 1987 ± 5 Ma and 1964 ± 4 Ma (Mänttäri 2010b), and the younger Mubende-Singo Suite with a U/Pb zircon age of 1848 ± 6 Ma (Mänttäri 2009) and an Rb/Sr age on biotite of 1.8 Ga (Nagudi *et al.* 2003).

Overlying the Rwenzori fold belt are sedimentary sequences belonging to the Paleoproterozoic post-Rwenzori platform sedimentary rocks and the Mesoproterozoic North Kibaran belt (Baglow *et al.* 2011). The accumulation of the Paleoproterozoic platform deposits

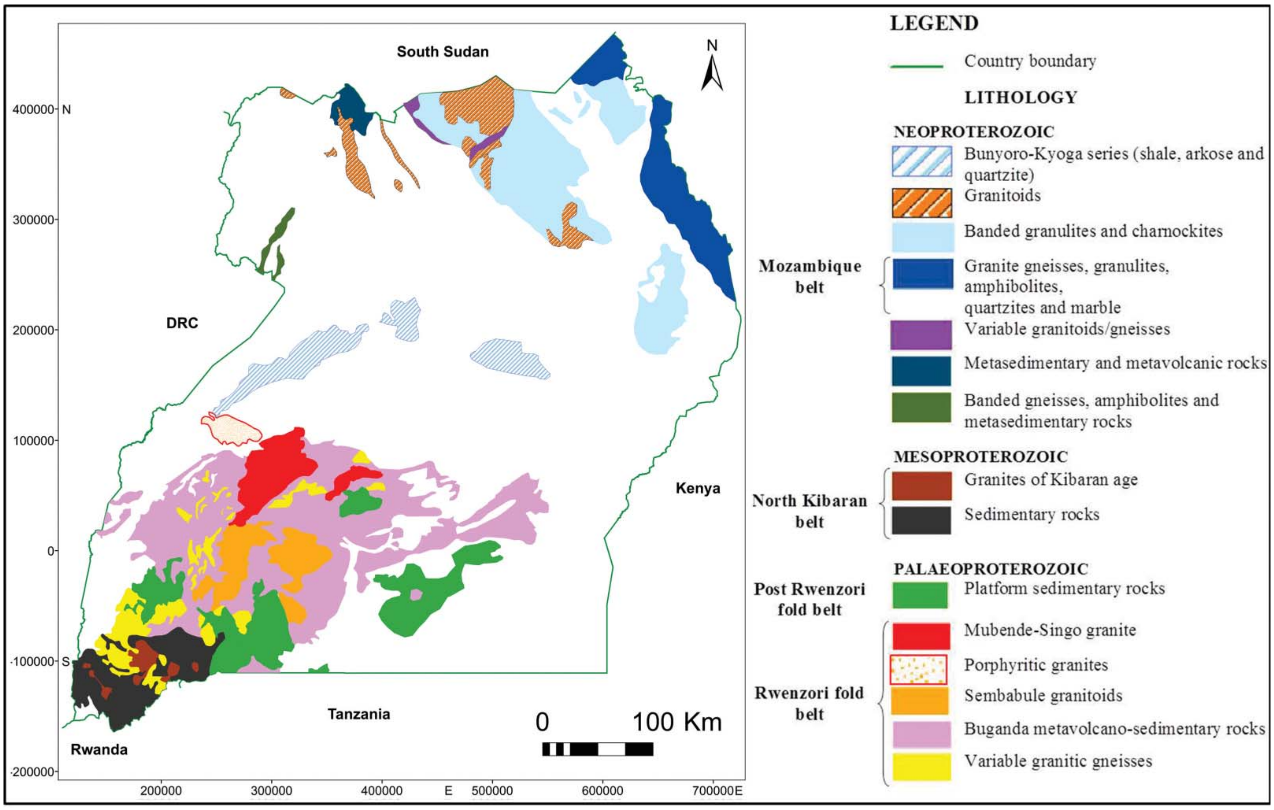

Figure 3 Geological map of Uganda displaying the Proterozoic lithologies. The map was constructed using available geochronological datasets of Uganda including Hepworth & Macdonald (1966), Schlüter & Hampton (1997), Begg *et al.* (2009), Elepu *et al.* (2011a), Mänttäri (2010a, b, 2011), Baglow *et al.* (2011, 2012a, b), and De Kock *et al.* (2012).

commenced after greenschist facies metamorphism and deformation of the Rwenzori fold belt, between 2.05 Ga and 1.78 Ga (Cutten *et al.* 2004).

The Mesoproterozoic sedimentary sequence (North Kibaran belt) is observed in Burundi, Rwanda, western Tanzania and Uganda. In Burundi, it is also known as the Burundian, whereas in Uganda and Tanzania it is alternatively known as the Karagwe-Ankolean system (Schlüter & Hampton 1997). This intra-cratonic fold belt comprises a thick Mesoproterozoic (1.53 Ga) succession, over 10 km in thickness, of mainly terrigenous folded and metamorphosed sedimentary rocks (Tack *et al.* 1994).

Extension in the North Kibaran belt culminated during a relatively short interval between 1380 and 1375 Ma with the emplacement of the North Kibaran Igneous Province (Tack *et al.* 2009). This extension was caused by a thermal (mantle) anomaly, giving rise to coeval bimodal magmatism, and represented by abundant S-type, peraluminous granitoids, subordinate felsic volcanics rocks (tuffs and lavas) and mafic subvolcanic rocks/mafic dykes and sills (Mäkitie *et al.* 2011a). Late orogenic granitoids (Mubende-Singo granites, 11) were emplaced into the metasedimentary rocks of the Buganda Group (Elepu *et al.* 2011a).

The Neoproterozoic geological events in Uganda are attributed to the N–S-trending Mozambique orogenic belt of East Africa. This generally contains polydeformed high-grade metamorphic rocks, with protoliths made up of predominantly older Mesoproterozoic to Archean continental crust that was strongly reworked during the Neoproterozoic (Stern 1994). This belt outcrops in the Karamoja area in the NE Uganda, and comprises a succession of metasedimentary rocks with minor igneous intrusions (Figure 3). All rocks have been metamorphosed at high pressure and temperature, and are now represented by granite gneiss and granulite with lenses of metasedimentary and metavolcanic rock (Baguma 2001).

Apart from the W- and SW-directed thrusting during the Pan African events, the NE corner of the Northern Uganda Terrane moved northwards, resulting in the development of the sinistral Aswa shear zone (Baglow *et al.* 2012a). The sinistral, strike-slip faulting within the Aswa shear zone has been estimated to have taken place at 0.69 Ga (Elepu *et al.* 2012). Emplacement of granitoids with a U–Pb zircon age of 659 ± 15 and 656 ± 16 Ma (Mänttäri 2010b), in the northern most part of Uganda (Figure 4), is tentatively attributed to this event.

The E–W-trending rocks of the Bunyoro-Kyoga series (Figure 3) are attributed to the Malagarasi Supergroup, a Neoproterozoic succession, of undeformed platform sedimentary rocks. The type locality was deposited in an intra-continental conjugate strike-slip basin (Tack *et al.* 1994), located in western Tanzania and eastern Burundi. The rocks of Bunyoro-Kyoga series (shale, arkose and quartzite) have been affected by weak deformation and commonly show distinct tilting (Hepworth & Macdonald 1966).

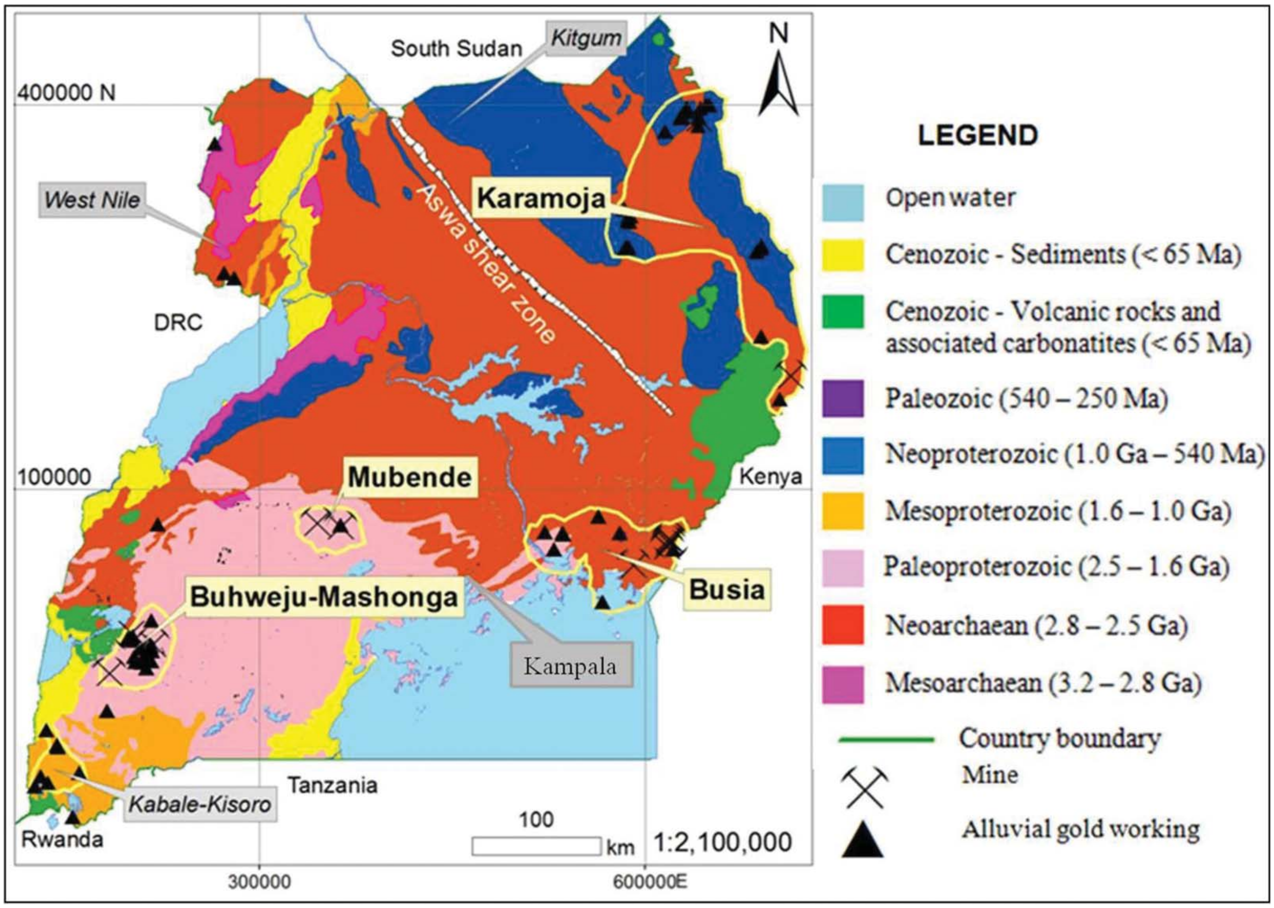

Figure 4 Geological map of Uganda showing the proposed locations of gold districts and other areas where alluvial gold mining and/or significant gold soil/rock chip values were reported. The geological map is based on Figure 1.

HISTORIC GOLD ASSESSMENT IN UGANDA

Historically, there are only limited scientific investigations about the gold districts in Uganda. Unpublished reports on gold occurrences from the Ugandan Department of Geological Survey and Mines (DGSM) date back to 1906, and gold was reported in the Paleoproterozoic metasedimentary rocks of western Uganda. The following summary on gold in Uganda is based on an extensive literature search, information and reports provided by selected gold exploration and mining companies operating in some of the districts, and interpretations based on field investigations and sample collections from a range of gold districts.

Wayland (1937) reported the discovery of alluvial gold along the foot of the Rwenzori Mountains in Kasese, SW Uganda (Figure 4). Simmons (1936) described alluvial gold workings in the valleys and rivers, and carried out geological investigations that led to the discovery of a quartz reef carrying gold. Gold was also recovered as a by-product during copper mining, which began in 1956 at the Kilembe mine in Kasese. Geological reports by Combe (1933, 1939), Roberts (1940), King (1941) and Barnes (1961) indicated several alluvial and quartz-vein gold discoveries and the presence of artisanal workings in the Paleoproterozoic and Mesoproterozoic rocks in SW Uganda. Follow-up work by prospecting and exploration companies led to the discovery of significant gold and base metal anomalies (Lytham 1965, 1967) over deposits that are now being mined by artisanal miners and small companies. Davis (1934) discovered gold-bearing quartz lodes in the Busia-Kakamega greenstone belt located in the Busia gold district (Figure 4). Exploration for primary gold in this area carried out between 1936 and 1939 led to the discovery of auriferous quartz veins in the currently operating Tira mine, and since then gold has been mined in several locations within the greenstone belt by both artisanal miners (open pit and alluvial mines) and small mining companies (open pit and underground mines). Biggs (1950) first reported gossan-associated base metal and gold occurrences in the Kalere River valley located in the Karamoja area. Since then, artisanal gold workings have been developed on alluvial gold occurrences in many of the streams in the Karamoja area and on less common colluvial gold locations (Baguma 2001). Barnes (1961) provided a summary of the mineral resources of Uganda including a section on gold mineralisation. Macdonald (1963) reported gold in streams extending from the River Nile to near the Uganda–DRC border. Alluvial gold in the West Nile region was reported by Harris (1942), and according to Otika (1960), alluvial gold in this region can be correlated with the auriferous Kibalian itabarites of Kilo Moto in the DRC from where the river flows.

In 1993–1994, a United Nations Development Programme (UNDP) project carried out a regional geochemical survey in the Buhweju areas (Pekkala *et al.* 1995). The samples collected were analysed for major and trace elements, and several high Au values of up to 1000 ppb were identified (Salminen *et al.* 2011).

The Geological Survey of Finland (GTK) Consortium, consisting of the GTK (the leading partner), GAF AG from Germany, Council for Geoscience (CGS) from South Africa, Faculty of Geo-information and Earth Observation of the University of Twente (ITC) from the Netherlands and Fels Consultants from Uganda carried out geochemical surveys and mineral resources assessment in selected areas of Uganda, from 2008 to 2012. The results of this project included the identification of potential gold mineralisation target areas including: (1) the West Nile Arua area, the extension of the Kilo Moto greenstone belt in the DRC through a stream sediment survey, (2) the Kitaka-Buhweju area in the Rwenzori fold belt through geochemical survey, (3) the Hoima area in the contact zone between the Neoproterozoic Bunyoro sedimentary rocks and Archean basement through stream sediment survey, and (4) the Aboke-Aloi area near the Aswa shear zone through geochemical and conceptual structural analysis (GTK Consortium 2012). Significant reports relating to gold mineralisation include Backman *et al.* (2011), Lehto *et al.* (2011), Lindh *et al.* (2011) and Manninen *et al.* (2011).

GOLD DISTRICTS IN UGANDA

This paper defines gold districts in Uganda based on the location of abandoned and active gold mines, workings, Au rock chip and soil anomalies, tectonic setting, geochronology, structures, and style of reported and observed gold mineralisation. The definition of the districts is preliminary, since in most areas only limited information on the geological setting and style of gold mineralisation is available. The four major gold districts in Uganda are: (1) the Busia gold district hosted in the Neoarchean Busia-Kakamega granite–greenstone belt in the SE of Uganda, (2) the Mubende gold district in the Paleoproterozoic Rwenzori fold belt in central Uganda, (3) the Buhweju-Mashonga gold district in SW Uganda, and (4) the Karamoja gold district hosted in reworked Archean basement rocks and/or in the upper amphibolite–lower granulite facies rocks of the Neoproterozoic Mozambique fold belt in NE and W Uganda. The gold districts are described in terms of their lithostratigraphic and structural setting, regional metamorphism, magmatism, and (regional) alteration; brief descriptions of the geological setting of gold mines and workings, including whole-rock and trace-element geochemistry of selected mineralised rocks are also provided.

Other regions in Uganda where alluvial gold mineralisation, shallow gold workings and/or rock chip or soil anomalies are reported include the Kitikum region, hosted in the Neoproterozoic Mozambique fold belt in the NE of Uganda; the Western Nile region, which represents the western extremity of the Bomu-Kibalian shield of NE Congo; NW Uganda; and the Kabale-Kisoro region, hosted in the Mesoproterozoic North Kibaran fold belt, in SW Uganda. These areas are presently not defined as gold districts owing to the lack of historic or active gold mines and the dearth of geological and mineralogical information. The southern Karamoja gold district and alluvial workings in the Kabale-Kisoro area were not visited during fieldwork owing to logistical limitations.

Busia gold district

The Busia gold district is located approximately 214 km from Kampala in SE Uganda (Figure 4). The geology of the area encompasses rocks of the Neoarchean Busia-Kakamega greenstone belt sequences (Nyanzian and Kavirondian Supergroups; 2.7–2.5 Ga; Gabert 1990) intruded by pre- and post-tectonic Neoarchean granites and granitoids. Metasedimentary rocks belonging to the Paleoproterozic Rwenzori fold belt and volcanic rocks of the East African Rift System (EARS) border the Busia gold district in the SW and NE, respectively (Figure 5).

There are limited published geological investigations and scientific papers defining the lithological units of the Busia gold district. Davis (1956) described the geology of part of SE Uganda with special reference to the alkaline complexes. Gabert (1990) reviewed the Archean cratons of Tanzania and SW Uganda in terms of their lithostratigraphy and tectonometamorphic events, and defined the main lithological units of the Busia-Kakamega greenstone belt.

STRUCTURAL SETTING, REGIONAL METAMORPHISM AND ALTERATION

All rocks in the Busia gold district have experienced relatively late movement on steep faults, most of which trend approximately NE–SW (Figures 5, 6). The metavolcanic rocks of the Nyanzian and Kavirondian supergroups in the Busia gold district generally strike in the NE–SW direction with subvertical to vertical dips. Structural analysis of the Archean greenstone belt in northern Tanziania, SE of the Busia gold district, indicated that layers of greenstone rocks are folded and display a regional fold axis with a plunge of 40°/320° (Bonifacel & Mruma 2012).

According to Old (1968) and Tanner (1973), the rocks of the Nyanzian Supergroup are metamorphosed to greenschist facies conditions with regional development of chlorite and biotite. Low-grade metamorphic mineral assemblages (actinolite–epidote–chlorite in basalts and muscovite–epidote–chlorite in granitoids) are common in the rocks of the Busia gold district and indicate a regional metamorphism at greenschist facies. However, BIFs and basalts are locally metamorphosed to epidote–amphibolite and amphibolite facies.

GOLD MINERALISATION

Gold was first discovered in the Busia gold district in 1932 in the Osipiri area (Combe 1933). Small-scale mining operations on vein and alluvial deposits began soon after this discovery and are ongoing at present. According to Harris (1961), the majority of known gold quartz vein deposits are epigenetic, hosted in carbonate-altered

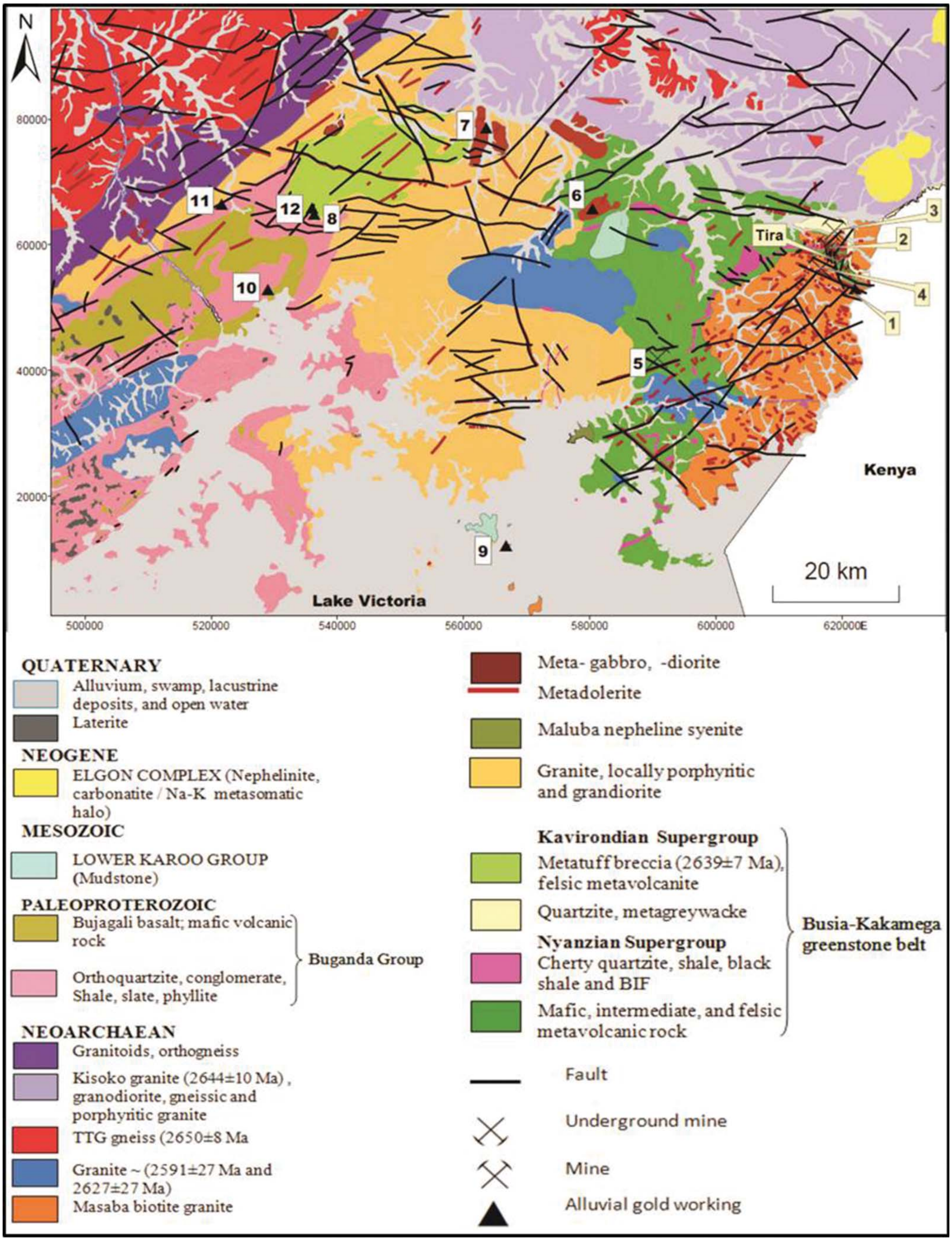

Figure 5 Geological map of the Busia gold district (modified after Davies 1934; Elepu *et al.* 2011a; Lindh *et al.* 2011). Mines: 1, Osapiri; 2, Amonikakinei; 3, Makina; 4, Busia Roraima; 5, Bude-Kitoja; 6, Bukiriri; 7, Butamakita; 8, Bulomba valley; 9, Kaza Island; 10, Mwiri-Walube valley; 11, Kagoma ridge; 12, Nakatama valley.

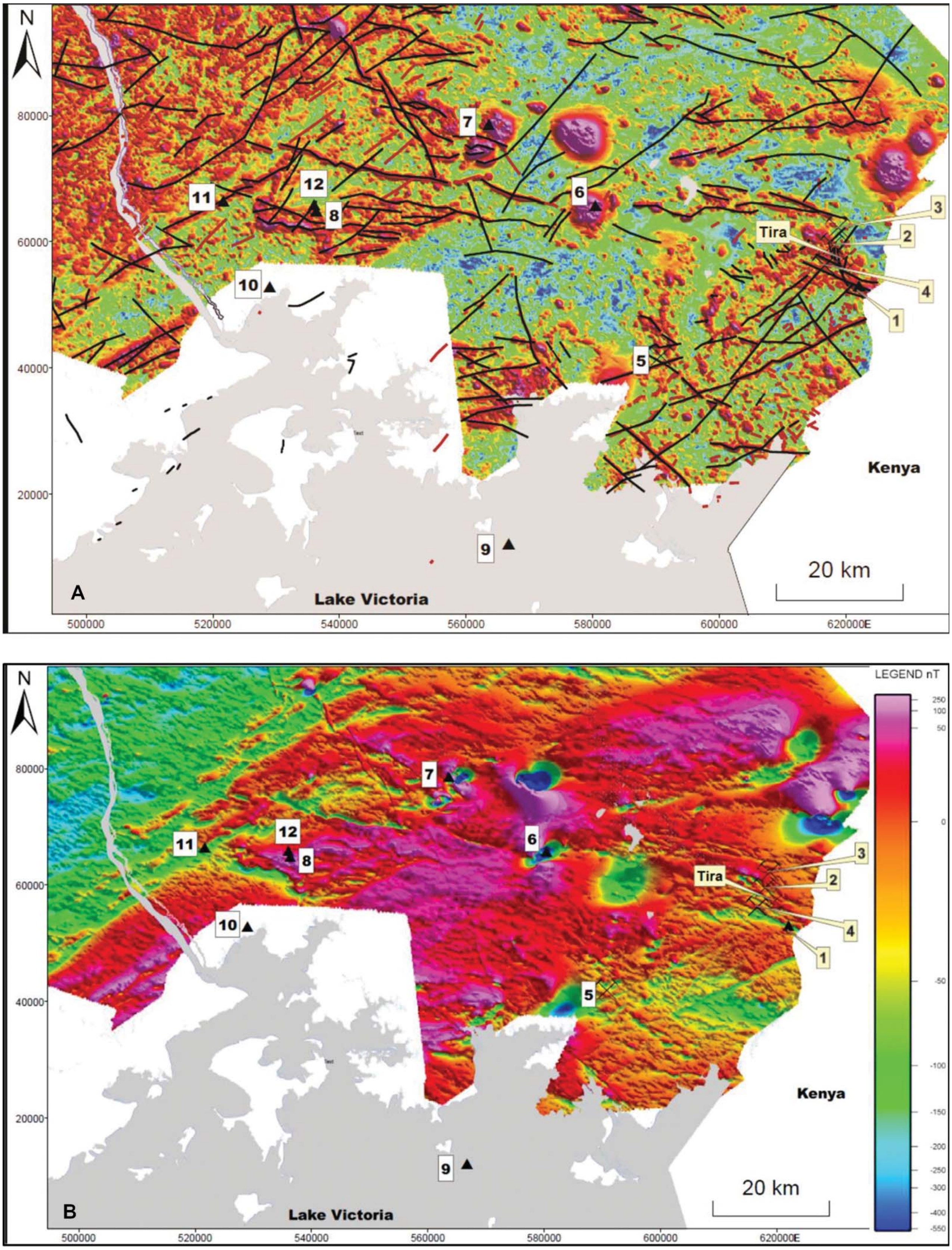

Figure 6 (a, b) Geophysical maps of Busia gold district. Airborne magnetic and electromagnetic surveys acquired by Fugro Airborne Surveys between 2006 and 2008, Department of Geological Survey and Mines, Uganda. Survey flight lines with a spacing of 200 m were flown in a NE–SW direction and tie lines with a spacing of 2000 m in a NW–SE direction, and were conducted with mean terrain clearance of 80 m and with a sample interval of 0.1 s and 1 s for magnetic and radiometric data, respectively. (A) Analytical signal map. (B) Aeromagnetic intensity signatures. Numbers indicate location of mines, see Figure 5 for explanation.

mafic metavolcanic rocks, and occur as structurally controlled quartz veins (reefs) in mineralised shear zones. Harris (1961) also suggested that in supracrustal rocks, alluvial gold is derived from weathered auriferous quartz veins, which may be related to late orogenic granitic activity. The Tira gold mine, located in the east of the Busia gold district (Figure 5), is the main mine in the Busia gold district and the only active underground gold mine in Uganda. There are several other localities in the Busia gold district, shown in Figure 5, where gold has been exploited. In the Amonkakinei area, about 10 km N of the Tira mine, artisanal miners exploit quartz reefs in several shallow open pits with at least seven parallel veins observed within a width of 1 km and a strike length of 6–7 km. Individual veins are about 0.4 m wide and located in weathered metadolerite and/or metasedimentary rocks.

TIRA MINE

The Tira gold mine was first operated by the Colonials as an open pit and underground mine (Schumann 2007). Within that period, two shafts were sunk, one on the New Reef (40 m below surface) and one near the Davis Reef reaching a depth of 131 m (Figure 7). Crosscut shafts were developed on two levels to intersect the two main branches of the Davis Reef. However, the mine became unprofitable and was closed in 1949. In 1991, the French Geological Survey (BGRM) carried out geochemical, alluvial and outcrop sampling. From 1994 to 1998, Anglo American Prospecting Services carried out surface sampling and drilling, and Roraima Mining Co Ltd conducted an exploration program including surface sampling, trenching, drilling and a geophysical survey. Busitema Mining CIE Ltd presently owns the mine and has been exploiting parts of the underground mine and carrying out exploration (Schumann 2007). The Tira Gold mine has been operating in Busia district since 1994, producing about 3 kg of gold a month (Ibrahim 2010).

The Tira mine is hosted by metasedimentary rocks, metabasalt and metadolerite. The metasedimentary rocks consist of metamorphosed shale, phyllite, sandstone and quartzite. The metabasalt is fine-grained, greenish grey cryptocrystalline and consists of chlorite, plagioclase, calcite, relict pyroxene and traces of rutile; locally, pyrite, either disseminated or within <1 mm wide veinlets, is observed. The metadolerite ranges from fine- to medium-grained, is locally foliated and contains plagioclase, quartz and chlorite-altered amphiboles. The contact between the metadolerite and the granite generally strikes in a NW–SE to NNW–SSE direction. The granite is intruded by a younger medium- to coarse-grained granite, which displays an equigranular texture consisting of K-feldspar, quartz, biotite and muscovite (Schumann 2007). The granite and the metadolerites have been crosscut by NE–SW-trending aplite dykes (Figure 7) that show a fine- to medium-grained equigranular texture, containing quartz, feldspar and muscovite, and an unidentified oxide mineral.

Gold mineralisation is structurally controlled by several NW- and NS-trending, subvertical to vertical ductile shear zones that contain locally massive, up to 2 m wide, shear zone-parallel quartz veins (reefs). Locally, the shear zone contains numerous small veinlets, which are locally termed stringer vein sets. The strong shear zone foliation can reach up to several metres into the surrounding wallrocks. The larger reefs displayed in Figure 7 have been named: (1) Davis Reef East, (2) Davis Reef West, (3) Samuels Reef, (4) MacAllister Reef and (5) New Reef. The NW-trending Davis Reef East, Davis Reef West and Samuels Reef are connected via underground levels and accessed via shaft 7 (Figure 7). The Davis Reef is also exploited in an up to 50 m deep open pit, the largest in the Tira mine, and includes a 1–1.5 m wide quartz vein with an average Au content of >10 g/t, the highest values exceeding 200 g/t (Schumann 2007). A second shaft (New Shaft), 47 m deep, accesses the NW-trending New Reef, which is also exploited in a large but shallow open pit (Figure 7). Based on analyses from trenches and diamond holes, the gold content of the New Reef is erratic, ranging from 2 to 10 g/t Au (Schumann 2007). The N–S-trending MacAllister reef is exploited by a series of open pits (Figure 7) and hosted in both metadolerite and metasedimentray rocks (Figure 7). The shear zone that hosts the quartz reef displays significant structural complexities with intersecting, overstepping fault-reef segments. Locally, parts of the reef terminate as small (<1 m wide) irregular swarms of stringer veins (Figure 7).

The quartz veins that constitute the main ore body are generally microfractured, smoky-white and cryptocrystalline to fine-grained, and consist of mainly quartz and calcite (Figure 8D–F). The quartz grains are subhedral to euhedral and <0.3 mm in size, and exhibit distinct undulating extinction; locally, quartz is sericitised along grain margins. Calcite is intergrown with quartz filling the fractures and voids, and forming <0.1 mm veinlets. Greenish grey massive chlorite forms along quartz grain margins with sericite grains and fill fractures and voids in the quartz. Boxwork textures are common and are locally filled by limonite.

The ore minerals in the quartz veins define thinly laminated sulfide veinlets that crosscut quartz, commonly parallel to foliation and consist of pyrite–hematite ± chalcopyrite ± gold (Figure 8C). The pyrite crystals are anhedral to subhedral and <0.3 mm, and overprint quartz and calcite along grain margins. Cubic crystals of hematite <0.2 mm and veinlets also overprint the main fabric and are intergrown with pyrite. Locally, fine-grained, brecciated crystals of pyrite overprint quartz, chlorite and sericite in the groundmass and fill fractures and voids in quartz. Locally, chalcopyrite and gold are intergranular in pyrite grains (Figure 8E, F).

The wallrock surrounding the quartz veins consists of foliated, fine-grained, hydrothermally altered metadolerite, metabasalt and metagabbro (Figure 8A, B). These rocks consist of quartz, plagioclase, biotite, hornblende, pyroxene and amphiboles, and are generally chlorite–carbonate altered. Anhedral crystals of chlorite form along quartz grain margins and fractures, and locally form thin bands replacing biotite and amphiboles. The anhedral plagioclase grains are clouded by calcite, and locally calcite fills the fractures and voids and forms <0.1 mm thick veinlets in plagioclase. Other minerals

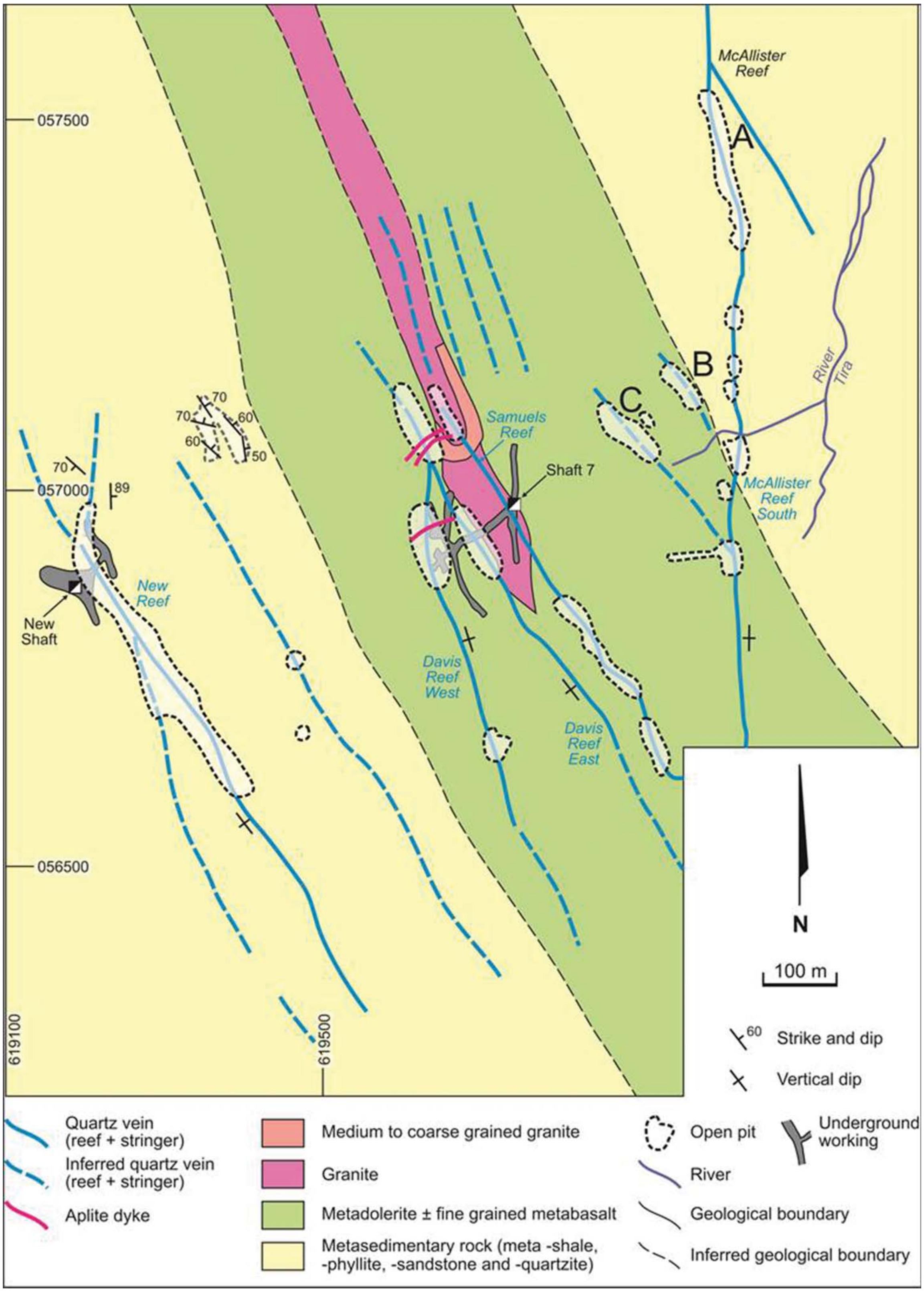

Figure 7 Geological map of the Tira mine; modified after Schumann (2007). A—Main MacAllister Pit; B—Eastern MacAllister pit; and C—Western MacAllister pit.

such as hornblende and biotite are partly replaced by chlorite. Locally traces of subhedral apatite, anhedral albite and subhedral rutile crystal are observed in quartz and plagioclase.

Whole-rock and trace-element analyses of hydrothermally altered rocks from the Tira mine (Table 1) revealed that hydrothermally altered metadolerite is high in $Fe_2O_{3(tot)}$ and moderately enriched in CaO

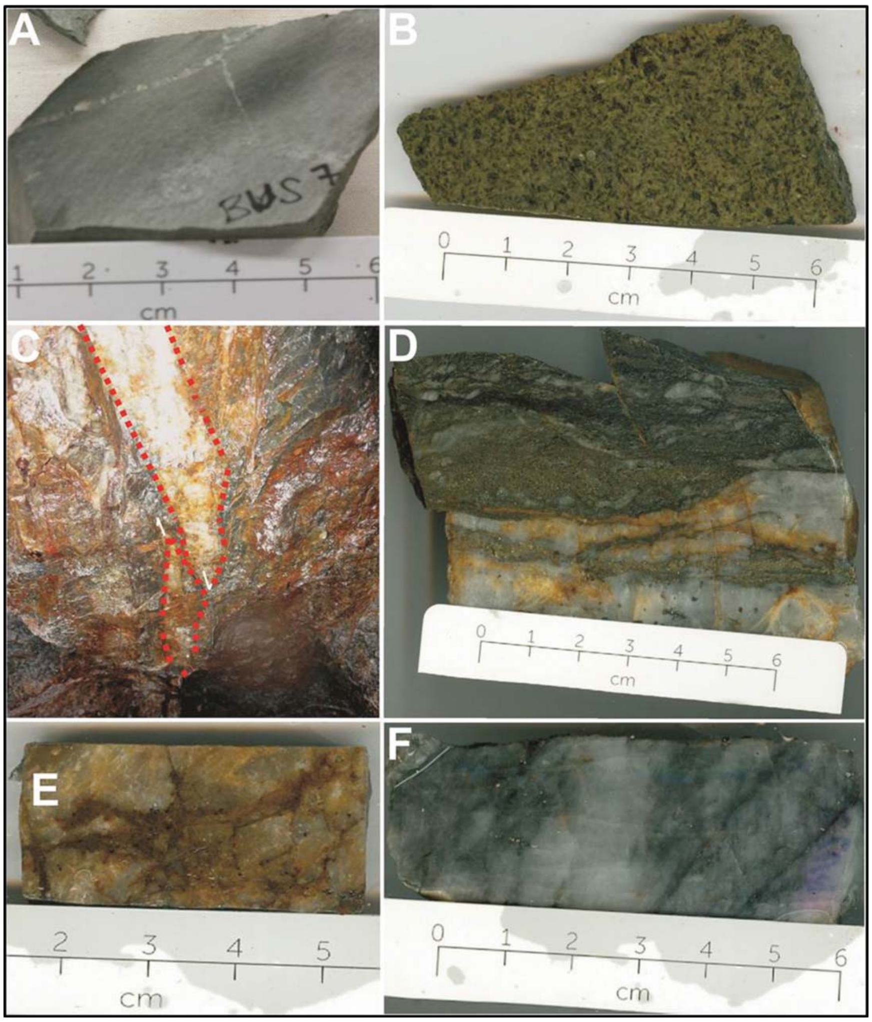

Figure 8 Photographs of hydrothermally altered rocks and veins from the Tira mine. (A) Chlorite–carbonate altered metabasalt. (B) Carbonate–chlorite altered metagabbro. (C) Quartz–carbonate shear vein parallel to the brittle-ductile shear zone that hosts and controls the ore body at the Tira underground mine. Note the small offset of the shear vein, suggesting minor, post-shear zone emplacement movement. (D) Contact of quartz–sulfide vein and hydrothermally altered (sulfidised) meta-dolerite wallrock. (E) Microfractured quartz vein cross-cut by sulfide veinlets. (F) Cryptocrystalline quartz–calcite vein cross-cut by chlorite and sulfide veinlets.

(samples BUS3 and BUS7, respectively) reflecting moderate carbonate and weak chlorite alteration. Sample BUS 4 displays high sulfur and gold contents, which are compatible with the intense sulfidation of the wallrocks at the margin with the mineralised quartz vein. The high Au content in sample BUS4 is associated with lower MgO, CaO, Na_2O and total C, but higher K_2O when compared with the low gold, and chlorite- and carbonate-altered wallrock samples (BUS 3 and BUS7). This is reflected in the replacement of amphiboles by sericite and pyrite, carbonate and plagioclase but slightly higher amounts of sericite in BUS 4.

With respect to metal zonation (Figures 9, 10) the Ag, As, Sb and S data both display a weak positive correlation with Au. In samples with Au>2 ppm, the Au–Ag ratio varies between 1.3 and 4.6. In terms of metal association, Au correlates positively with Mo+Bi+W+Li and Sn+W but only weakly with As+Sb and Cu+Pb+Zn. The metal-zonation pattern suggests that Au is associated with sulfides but also occurs as 'free' gold in the veins, which is supported by petrographic observations. The positive correlation of Au with the 'igneous' element associations (Mo+Bi+W+Li and Sn+W) suggests that some of the Au may have been derived from magmatic–hydrothermal fluids.

Mubende gold district

The Mubende gold district is located approximately 100 km west of Kampala in central Uganda (Figure 4). The regional geology of the Mubende gold district encompasses rocks belonging to the Buganda metavolcano-sedimentary rocks in the Paleoproterozoic Rwenzori fold belt (2.1 to 1.85 Ga) and sedimentary sequences of the Paleoproterozoic post-Rwenzori platform sedimentary rocks, deposited on Neoarchean basement gneisses (Elepu *et al.* 2011b). Late orogenic Mubende-Singo granites also belonging to the Buganda Group intruded the metasedimentary rocks (Figure 11). The entire area has been crosscut by a 1.4 Ga (using U/Pb on zircon; Mänttäri 2009) arcuate dolerite dyke swarm.

STRUCTURAL SETTING, REGIONAL METAMORPHISM AND ALTERATION

The prominent structures in the Mubende gold district are WNW–ESE-trending fault zones, which have been crosscut by NE–SW-trending faults with offsets of <80 m (Figure 11). The NE–SW-trending faults are offset by late NNE–SSW-trending faults (Figure 11). The Namuwasa Group, comprising orthoquartzite, shale, slate, phyllite,

Table 1 Whole rock major oxide (in wt%) and trace element (in ppm) analysis of selected samples from the Tira mine in the Busia gold district.

Sample No	**BUS 1**	**BUS 2**	**BUS 3**	**BUS 4**	**BUS 5**	**BUS 6**	**BUS 7**	**BUS 8**	**BUS 9**
Lithology	**metadol**	**metadol**	**metadol**	**metadol**	**metadol**	**metadol**	**metadol**	**metadol**	**metadol**
Sample analysed	**chl alt qtz–sul vein**	**qtz-carb vein**	**meta gabbro**	**chl alt qtz–sul vein ± ser**	**ser alt metadol**	**carb ± ser alt qtz ± sul vein**	**chl alt metabasalt**	**qtz–sul vein**	**qtz–carb–sul vein**
wt%									
SiO_2	na	na	56.37	73.97	na	na	45.60	na	na
Al_2O_3	na	na	15.24	5.29	na	na	15.40	na	na
Fe_2O_3(T)	na	na	7.33	9.15	na	na	14.50	na	na
MnO	na	na	0.12	0.14	na	na	0.25	na	na
MgO	na	na	3.63	0.54	na	na	6.32	na	na
CaO	na	na	4.57	0.96	na	na	5.10	na	na
Na_2O	na	na	4.62	0.47	na	na	3.42	na	na
K_2O	na	na	0.82	1.69	na	na	0.14	na	na
TiO_2	na	na	0.79	0.31	na	na	0.98	na	na
P_2O_5	na	na	0.36	0.07	na	na	0.08	na	na
LOI	na	na	5.29	5.23	na	na	7.51	na	na
Total	na	na	99.13	97.82	na	na	99.30	na	na
C-Total	na	na	0.70	0.20	na	na	1.07	na	na
S-Total (in ppm)	712	41	10	6430	8000	111	190	33	9
ppm									
Au	3.88	0.39	bdl	12.30	2.29	6.21	0.05	0.26	25.90
Ag	1.60	1.60	1.10	2.70	2.00	1.40	1.23	0.30	20.80
As	31.6	25.5	5.1	123.0	na	9.9	0.7	53.0	30.3
Sb	1.10	0.60	0.30	0.70	0.52	0.30	bdl	2.60	0.60
Hg	bdl	bdl	bdl	bdl	bdl	bdl	bdl	bdl	bdl
Te	na	na	0.7	1.6	0.4	na	bdl	na	na
Bi	na	na	0.15	29.4	0.30	na	0.16	na	na
Mo	bdl	bdl	0.7	9.9	4.3	13.0	0.3	3.0	bdl
Li	na	na	29.4	18.1	28.0	na	31.2	na	na
W	bdl	bdl	1.2	24	3.5	bdl	0.2	4.0	120
Sn	na	na	2	2	bdl	na	bdl	na	na
Cu	198	24	20	250	288	10	40	32	101
Pb	198	1140	13	485	139	42	3	21	404
Zn	212	54	100	320	112	16	100	14	26
Cr	na	na	100	90	bdl	na	170	na	na
Ni	15	19	40	20	16	8	150	8	17
Co	na	na	19.9	65.1	6.0	na	46.3	na	na
V	na	na	127	123	120	na	312	na	na
Au/Ag	2.43	0.25	<0.01[a]	4.56	1.15	4.44	0.04	0.86	1.25
Au/Cu	0.02	0.02	<0.01[a]	0.05	<0.01[a]	0.62	<0.01[a]	<0.01[a]	0.26
As+Sb	33	26	5	124	–	10	1	56	31
Mo+Bi+W+Li	–	–	31	81	36	–	32	–	–
Sn+W	–	–	3	26	5	–	1	–	–
Cu+Pb+Zn	608	1218	133	1055	539	68	143	67	531
Cs	na	na	2.67	2.49	2.70	na	1.69	na	na
Rb	na	na	23.5	36.1	32.6	na	3.8	na	na
Ba	bdl	bdl	402	988	648	140	60	140	bdl
Sr	na	na	395	40	83	na	92	na	na
Th	na	na	6.50	1.80	5.10	na	0.30	na	na
U	na	na	1.8	0.5	1.2	na	bdl	na	na
Zr	na	na	141	71	145	na	50	na	na
Hf	na	na	3.5	1.4	1.8	na	0.3	na	na
Nb	na	na	6.0	2.0	na	na	2.0	na	na
Ta	na	na	0.4	0.2	0.3	na	0.1	na	na
Sc	na	na	15	7	8	na	39	na	na
Y	na	na	18	4	11	na	16	na	na
Se	na	na	1.3	1.4	bdl	na	0.7	na	na
Be	na	na	2.3	0.7	na	na	0.4	na	na
Cd	7.8	1.9	0.3	12.0	3.0	bdl	bdl	0.7	0.5
Ga	na	na	20.8	9.8	na	na	18.2	na	na
Ge	na	na	2	2	na	na	2	na	na
In	na	na	bdl	0.30	0.04	na	bdl	na	na
Re	na	na	0.009	0.003	bdl	na	0.004	na	na
Tl	na	na	0.13	0.16	0.20	na	bdl	na	na

sul, sulfide; ser, sericite; carb, carbonate; bdl, below detection limit; na, not analysed.

Note: [a]Detection limit value use to calculated the ratio; –, not calculated.

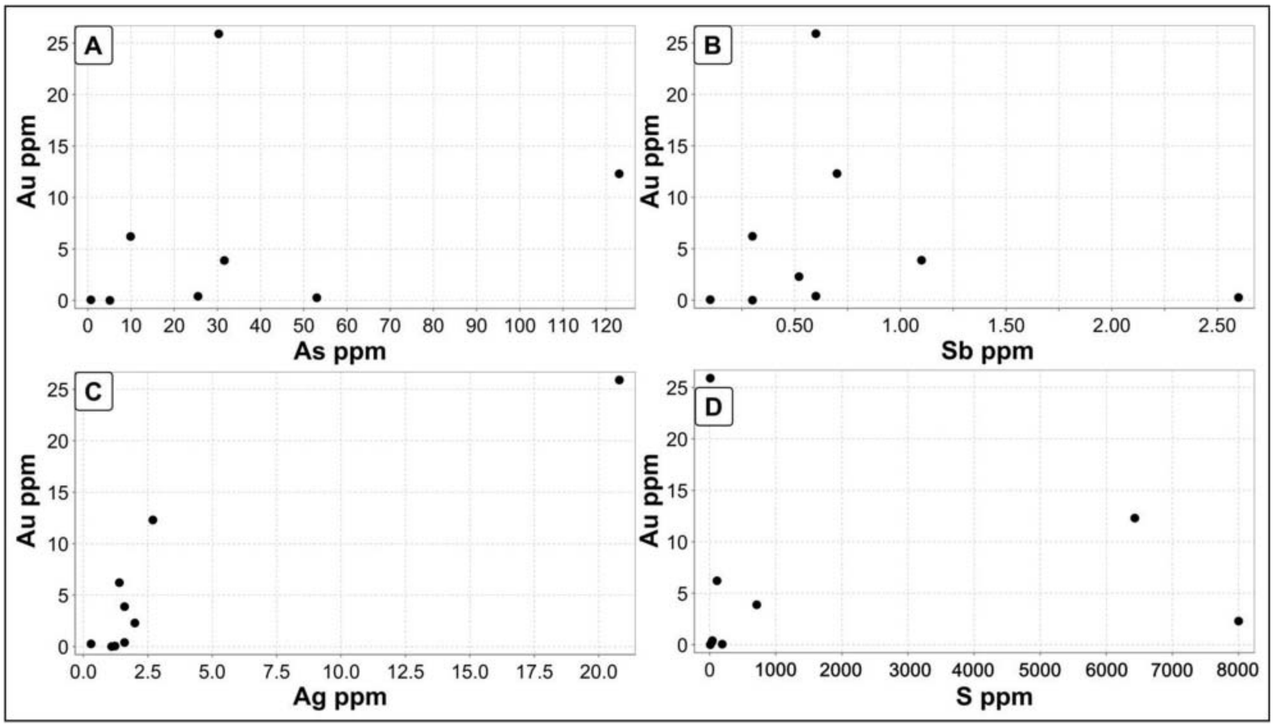

Figure 9 Multi-element diagram of Au *vs* As (A), Au *vs* Sb (B), Au *vs* Ag (C), and Au *vs* S (D) from hydrothermally altered and mineralised samples from the Tira underground mine.

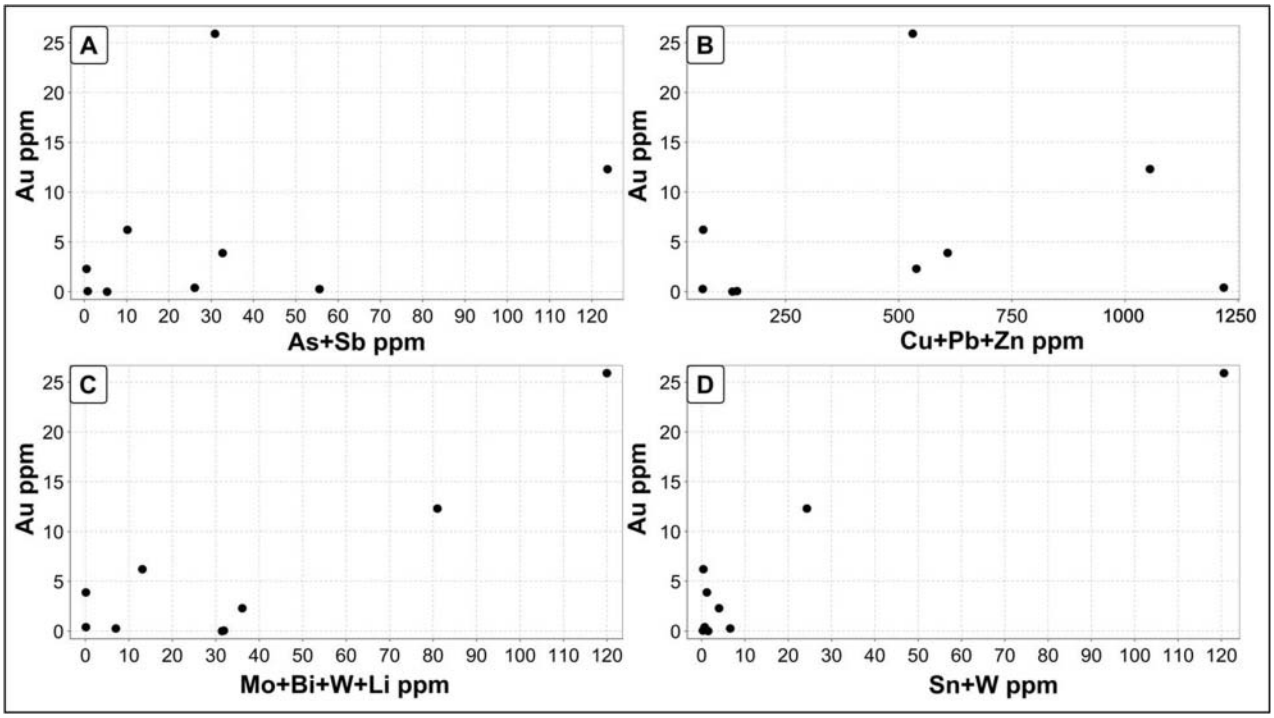

Figure 10 Multi-element diagram of Au *vs* As+Sb (characteristic for orogenic gold deposits; A), Au *vs* Cu+Pb+Zn (base metals; B), Au *vs* Mo+Bi+W+Li (typical felsic magma-related elements; C), and Au *vs* Sn+W (typical reduced magma-related elements; D) from hydrothermally altered and mineralised samples from the Tira underground mine.

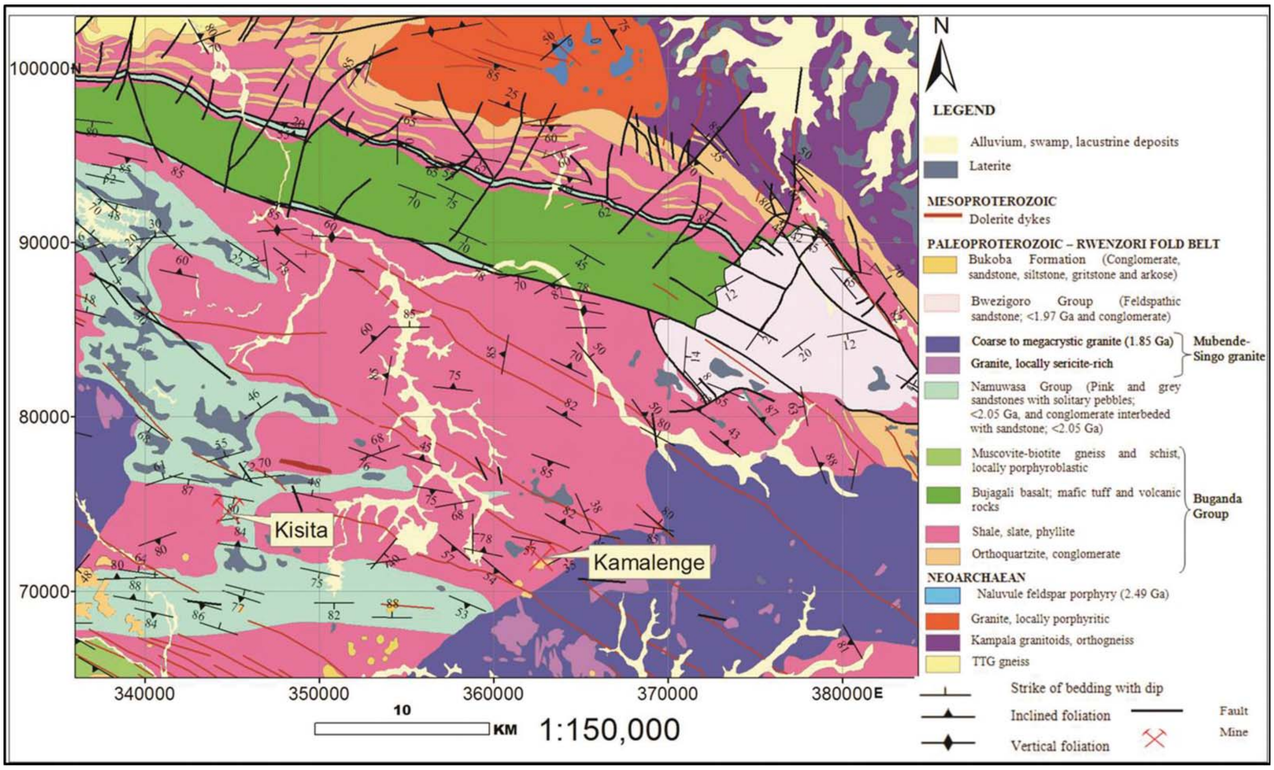

Figure 11 Geological map of the Mubende gold district; modified after Johnson & Williams (1961) and Mäkitie *et al.* (2011b).

muscovite–biotite gneiss and schist, generally retain a distinct foliation that trends NW–SE and dips vertically to 60°NE. The strike and dip of the bedding surfaces vary considerably and suggest that these rocks have been locally folded. According to Tanner (1973), the folded sequence of Paleoproterozic metasedimentary rocks is best preserved in elongated synclines and rest uncomfortably on the Archean gneiss. The Bujagali volcanic rocks are steeply dipping with a general strike of N40°W. The Mubende-Singo granites intrude the Paleoproterozoic rocks but are not affected by deformation or faulting and lack metamorphic minerals suggesting their emplacement is late, post-deformation in the Paleoproterozoic.

The regional metamorphic history of the rocks in the Mubende gold district has not been extensively studied, but according to Tanner (1973), pressure and temperature conditions in the Rwenzori fold are indicative of high thermal gradients. The schists within the Rwenzori fold belt are characterised by widespread cordierite with members of the Buganda Group metamorphosed under higher temperature conditions compared with the other metasedimentary units in the Mubende gold district. Most shale, slate and phyllite of the Buganda Group are characterised by metamorphic muscovite suggesting greenschist facies metamorphism. Elepu *et al.* (2011b) reports a contact metamorphic zone around the Mubendo-Singo granite.

GOLD MINERALISATION

The Mubende gold district contains the Kamalenge and Kisita gold mines, which are surrounded by numerous alluvial gold workings. There are several localities at the contact between the Singo granite and metasedimentary rocks where the granite is hydrothermally altered with weak to strong biotite–sericite–chlorite alteration. The timing relationship of this alteration to gold mineralisation is presently unknown.

KAMALENGE GOLD MINE

The Kamalenge gold mine is located in the S of the Mubende gold district, about 1 km from the contact of the Singo granite batholith (Figure 11). According to Data *et al.* (2009), gold has been mined at Kamalenge since 1948. These authors have reported a 50 m long adit and several alluvium gold workings within rivers and valleys near the Kamalenge mine. Baguma (1991) estimated the total gold reserves in the Kamalenge mine to be 2.45 tonnes. Since 1992, Anglo Ugandan Corporation (AUC) has been exploring for gold and base metals in the area.

The old, abandoned gold adit is hosted in metasandstone interbedded with silicified metashale, metaconglomerate and metasiltstone, and controlled by a shear zone with a strike of N60°W and dip of 60°SW. This shear zone contains quartz–hematite ± albite veins; the wall rocks at the contact to these veins are silicified. There is a second, minor shear zone with a strike of N48°E and a dip of 46°NW. The direction of the main, 20 m long and 2 m wide, adit follows the trend of the main shear zone.

The quartz–hematite ± albite veins are characterised by subhedral to euhedral granular and hydrothermal specular hematite, with lamella twinning, filling the cracks and spaces within the quartz ± albite grains. Rare albite grains are in equilibrium with quartz. Brown subrounded grains of ilmenite locally overprint the granular hematite grains.

Hydrothermally altered and mineralised, fine- to medium-grained metashale and metasandstone are characterised by a yellowish grey, pink to reddish brown colour, with relict detrital quartz and plagioclase as well as abundant hydrothermal albite, sericite, hematite and traces of rutile and tourmaline. Late-stage muscovite (<0.3 mm) overprints the earlier fabric and the hydrothermal alteration minerals. The diamond-shaped euhedral hematite grains are disseminated within the wallrock and as anhedral grains (<0.1 mm) in fractures and voids. The hematite contains pleochroic inclusions of magnetite ± pyrite, indicating that the hematite has replaced magnetite and possibly sulfides (<0.3 mm).

KISITA GOLD MINE

The Kisita gold mine is located in the SE of the Mubende gold district, approximately 8 km E of the Singo granite and 18 km west of the Mubende granite (Figure 11). The Kiboga Kyakiddu Mining Company carried out gold exploration at the Kisita gold mine in 1996. Presently, Kisita Mining Co. Ltd is conducting gold exploration and exploits alluvium gold. Carr (2002) reported a total *in situ* reserve of 1 612 500 tonnes at 8.33 g/t Au for the Kisita mine; the nearby alluvial reserve is 1 200 000 tonnes at 6.66 g/t Au. Gold mineralisation at the Kisita mine is hosted in fine-grained metasandstone, metashale and metaconglomerate similar to the gold in the Kamalenge mine (Data *et al.* 2009).

Buhweju-Mashonga gold district

The Buhweju-Mashoga gold district is located approximately 330 km from Kampala in SW Uganda (Figure 4). The geology of the Buhweju-Mashoga gold district is characterised by Paleoproterozoic rocks of the Rwenzori fold belt and the platform sedimentary rocks of the post-Rwenzori fold belt (terminology after Baglow *et al.* 2011). Other lithological units in the district include Mesoproterozoic dolerite dykes generally trending NW–SE, and Neogene volcanic rocks and sediments deposited on the western branch of the EARS.

STRUCTURAL SETTING, REGIONAL METAMORPHISM AND ALTERATION

The Rwenzori fold belt and post-Rwenzori fold belt have been deformed by complex fault and shear zones and several generations of foliations (Schlüter & Hampton 1997). The metasedimentary rocks of the Buganda Group retain a distinct foliation that trends NE–SW and dips nearly vertically to 45°NW (Figure 12). The strike and dip of the bedding surfaces are variable, indicating potential folding of the strata.

Several faults in the Buhweju-Mashonga gold district offset the stratigraphy, and the most prominent vertical faults trend NE–SW with lithological offsets of <100 m. These faults are crosscut by late NNW–SSE- and NW–SE-trending subvertical faults (Figure 12).

Bahiru (2011) summarised the geological history and sequence of geological events of the area and suggested that the deposition of the Buganda Group was followed by regional-scale folding with fold axes trending northwards; this event was accompanied by greenschist facies regional metarmorphism, followed by deposition of the Kagera-Buhweju Supergroup. The rocks of the Kagera-Buhweju Supergroup were locally folded with fold axes trending WNW. This event caused the refolding of the Buganda Group rocks generating complex interference fold patterns.

GOLD MINERALISATION

The Buhweju-Mashonga gold district contains numerous gold mines (Figure 12) including the shallow open pits and adits of the Mashonga mine, adits in the Buckley's and Anderson's reefs, and underground stopes in the Kitaka mine. Unpublished reports at the Ugandan DGSM indicate that most of the gold production in Uganda comes from alluvial mining in the Buhweju-Mashonga areas where the source rock is not known (Data *et al.* 2009). According to Combe (1932), alluvial gold in this area was first mined in the valleys and streams within the quartzitic sandstone. Since then, alluvial gold has been exploited at Rwengwe, Bisya, Muti River, Chonyo River, Kampono, Nyamunyomwa River, Kitomi River, Kanywambogo, Kyangwahanda River and Nyakahita Valley (Figure 12). Limited scientific and/or company reports are available for all these localities.

KITAKA MINE

The Kitaka mine is located in the NW of the Buhweju-Mashonga gold district (Figure 12). This deposit was first described by Barnes (1961) who reported a sulfide-bearing (galena–chalcopyrite) quartz reef that contains gold. Cratchley & Evans (1967) suggested that the ore body (massive quartz vein with lead, copper and zinc sulfides) is located within a 40 m wide dolerite dyke that strikes N20°E and dips about 45°SE, and exhibits sheared contacts with the quartz–biotite gneiss it intruded. These authors also carried out an electromagnetic (EM) geophysical survey of the area and described a weak conductor within the mine, close to the dolerite dyke that may be caused by magnetisation of the dyke edges or by pyrrhotite, possibly associated with the dyke.

The Kitaka mine is located in metagranodiorite and metadolerite within a fault plane striking N20°E and dipping 40°SE in a brittle-ductile shear (Figure 13A). The metagranodiorite is dark grey–green and medium-grained, and contains quartz, hydrothermal chlorite, plagioclase, biotite as well as disseminated hydrothermal chalcopyrite–pyrite–galena. The quartz grains are subhedral and show undulating wavy extinction; plagioclase grains are locally sericitised particularly along cleavage planes (Figure 14A). Locally, euhedral monazite and apatite crystals are contained within plagioclase and quartz (Figure 14A). The flaky and fibrous biotite crystals are interlocked in quartz and feldspar grains and are replaced by massive hydrothermal chlorite (Figure 14B, C).

The metadolerite is fine-grained, greenish-grey and foliated, and contains quartz, plagioclase, biotite, as well as hydrothermal chlorite–sericite–carbonate ± sulfides

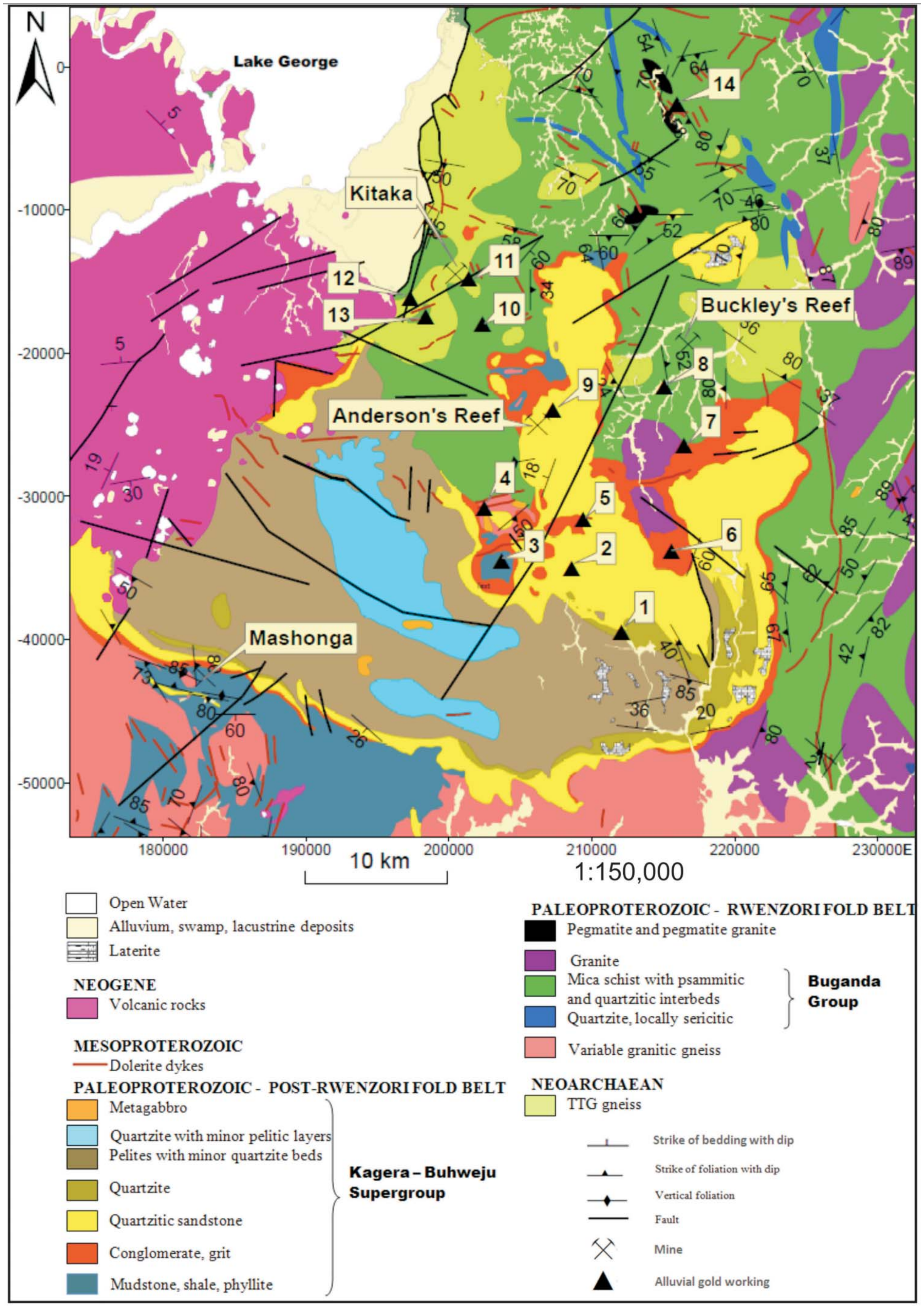

Figure 12 Geology map of the Buhweju-Mashonga gold district (modified after Reece 1961; Bahiru 2011; Mäkitie *et al.* 2011b) displaying the major gold mines. Also shown are alluvial gold workings: 1, Rwengwe; 2, Bisisa; 3, Katongo swamp; 4, Chonyo River; 5, Muti River; 6, Bisya; 7, Kirunga; 8, Kyangwahanda River; 9, Karembe; 10, Kanywambogo; 11, Kitomi River; 12, Nyamunyobwa River; 13, Kampono; 14, Nyakahita valley.

Figure 13 Photographs of the Kitaka mine area. (A) Photo taken towards the north showing a fault plane striking N20°E and dipping 40°SE. This fault zone appears to control the ore body at the Kitaka mine. (B) Hand sample of massive quartz–galena vein. (C, D) A network of hydrothermal quartz–carbonate veins hosting galena, chalcopyrite and pyrite. The green mineral is supergene malachite in chalcopyrite rich areas.

(Figure 14B). Locally, the biotite has been replaced by hydrothermal chlorite.

The mineralised zone consists of a network of hydrothermal quartz–carbonate–galena–chalcopyrite veins of possibly different ages (Figure 13B–D). The veins consist of quartz, plagioclase, chlorite, sericite, sulfides and carbonates (Figure 14D); locally the veins also contain clear quartz crystals. The main sulfides are galena–chalcopyrite–pyrite ± chalcocite ± pyrrhotite ± gold. Chalcocite replaces chalcopyrite along grain margins, and pyrrhotite occurs as inclusions in chalcopyrite (Figure 14E, F). Locally, hydrothermal anhedral to subhedral grains and veinlets of chalcopyrite–pyrite–galena replace quartz and plagioclase along grain margins and fill fractures and voids in the wallrock.

Geochemical analyses of hydrothermally altered granodiorite (Table 2) have high K_2O (KIT 2) and Na_2O (KIT 1 and KIT 4), which are associated with high modal sericite and plagioclase, respectively. Mineralised vein samples (KIT 3, KIT 5), and particularly KIT 6, contain high base metals, the latter sample also containing high Au and Ag values (11 and 116 ppm, respectively). All other metals such as As, Sb, Bi, Mo and Sn have low abundances. Lehto *et al.* (2011) present trace-element data for a massive galena lens from the main quartz vein in the Kitaka mine, including 66.1% Pb and 30.1 ppm Ag. A hydrothermally altered carbonate–chlorite rock containing disseminated galena (2.35% Pb) contains 8.4 ppm Ag, 1.79 ppm Au, 70–170 ppm Zn and 50–190 ppm Cu.

MASHONGA MINE

The Mashonga mine, located in the SW of the Buhweju-Mashonga gold district, was discovered by Combe in 1933 and exploited for gold by Kagera Mines Ltd in 1934 for one year (Data *et al.* 2009). Since then, gold has been exploited in shallow pits, and alluvial gold has also been mined from streams and valleys within the area, but no exploration reports and production records can be traced.

The geology of the Mashonga mine area is generally made up of mudstone, shale, slate and phyllite, which are overlain by quartzite and conglomerate (Figure 12). In a granite outcrop about 150 m in the SE from the major pit, a set of en-enchelon type quartz vein networks is related to the major shear (gold reef) that indicates that the prospective gold zone may be very large.

The gold reef, which is exploited in the shallow open pit, is controlled by an ENE–WSW-striking, subvertically dipping shear zone crosscutting through kaolinised granites and weathered muscovite schists. Locally, these rocks are mylonitised and contain quartz ± gold veins. Most silicates have been hydrothermally altered and overprinted likely during shearing, to a sericite–muscovite-rich rock (muscovite schist); other minerals include chlorite, sericite and hematite. Cubic pyrite crystals, which have been replaced by hematite, overprint the main foliation fabric.

The granite is medium-grained and equigranular, and locally contains euhedral quartz and muscovite phenocrysts. The typical mineral assemblages of quartz (kaolinised)–muscovite–chlorite–feldspar (K- and Na-rich) suggests that the granite has only been metamorphosed at a low metamorphic grade.

ALLUVIAL GOLD WORKINGS

The Muti River gold workings, located in the central area of the Buhweju-Mashonga gold district (Figure 12), are represented by alluvial gold in the streams and valleys, and quartz reefs in quartzitic sandstones. The area was first mapped by Combe (1933), who suggested that gold and pyrite in the area exists in a stock work of quartz stringers hosted in quartzites. However, the bulk of all

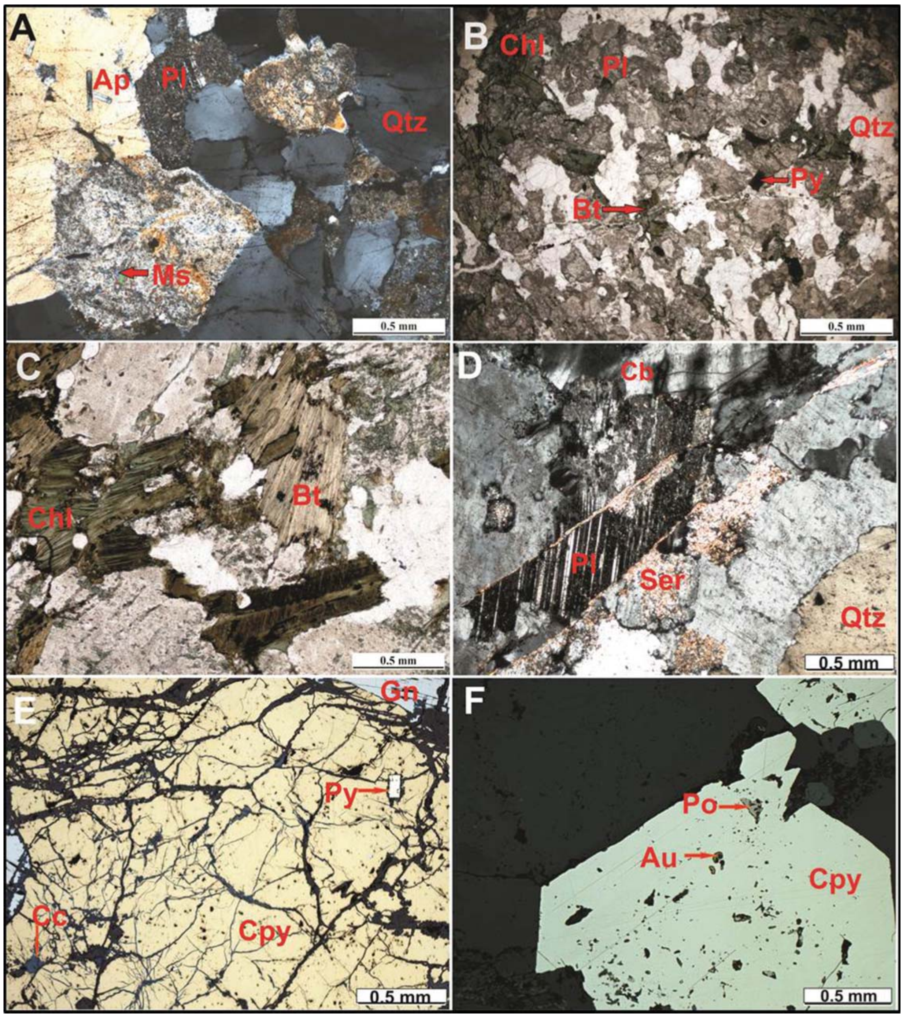

Figure 14 Photomicrographs of the host rocks and mineralised rocks from the Kitaka mine area. (A) Meta-granodiorite showing euhedral Ap-apatite crystals in Pl-plagioclase and Qtz-quartz, Ms-muscovite in plagioclase, and distinct undulose extinction in quartz. (B) Meta-dolerite consisting of intergrown plagioclase, quartz and Bt-biotite, and hydrothermal Chl-chlorite, Py-pyrite. (C) Hydrothermal replacement of the fibrous biotite by green chlorite in metagranodiorite. (D) Quartz Cb-carbonate vein consisting of hydrothermal Ser-sericite replacing plagioclase along grain margins. (E) Gn-galena and Cpy-chalcopyrite intergrown, pyrite interlocked in chalcopyrite, and Cc-chalcocite replaces chalcopyrite along grain margins. (F) Po-Pyrrhotite ± Au gold is disseminated in Cpy-chalcopyrite in a quartz–carbonate–galena–chalcopyrite vein.

gold from Muti was exploited from small but rich alluvial workings along the river banks, but no production record can be traced (Data *et al.* 2009). Wayland (1934) indicated the possibilities of 'crystalline gold' and of auriferous lodes in the vicinity of the Muti area. Reconnaissance geochemical exploration between 1992 and 1994 highlighted stream sediments with more than 100 ppb, and locally even more than 1000 ppb (Pekkala *et al.* 1995). The gold in the Muti mine area is hosted by quartzitic sandstone, conglomerate and grit overlying granite, which is exposed 4 km east of the Muti River workings (Figure 12). The quartzitic sandstone is poorly sorted; matrix supported, fine- to medium-grained, dark bluish/smoky and sericite-rich, with disseminated cubic pyrite crystals overprinting the main rock fabric. The quartzitic sandstone comprises a network of numerous quartz veins that includes plagioclase, rutile, tourmaline and large euhedral quartz crystals potentially indicating several periods of hydrothermal activity.

The Kanywambogo gold workings, located in the central area of the Buhweju-Mashonga gold district (Figure 12), consist of abandoned shallow adits, trenches and alluvial workings along streams and valleys. The mineralised area is located within a NE–SW striking, subvertical fault zone that has been crosscut by a younger shear zone with a strike of N60°W and a dip of 48°SE that controls the mineralised quartz vein. According to Data *et al.* (2009), the undeformed vein, hosted in the quartzite, consists of quartz ± chalcopyrite ± galena ± gold. Presently, at this locality, only a network of hydrothermal veins/breccias within quartzite interbeds is visible. Geochemical analysis of a quartz vein sample from Kanywambogo gave 5–10% Cu, 376 ppm Ni, 210 ppm Pb, 13.4 ppm Ag and trace amounts of Au and As. Geochemical analyses of three sulfide-bearing quartz veins from the Kanywambogo trench contain 0.1–1% Cu, up to 376 ppm Ni, 210 ppm Pb, and 13.4 ppm Ag.

Karamoja gold district

The Karamoja gold district, located in the NE of Uganda (Figure 4), was first mapped at a scale of 1:250 000 and published in the 'Geology of Karamoja' by Williams (1966). Macdonald (1961, 1966), Williams (1966), Elepu *et al.* (2012) and Baglow *et al.* (2012b) subdivided the rocks of the Karamoja gold district into the Karamoja and the Karasuk groups. The Karamoja Group is made up of a mixed assemblage of granite gneiss, migmatite, biotite gneiss, banded biotite and garnet gneiss, granulite and charnockite, leucocratic granite gneiss, and minor amphibolite. The Karasuk Group consists of a mixture of undifferentiated granite gneiss, quartzite

Table 2 Whole rock major oxide (in wt%) and trace element (in ppm) analysis of selected samples from the Kitaka mine in the Buhweju-Mashonga gold district.

Sample No	**KIT 1**	**KIT 2**	**KIT 3**	**KIT 4**	**KIT 5**	**KIT 6**
Lithology	**Least alt granodiorite**	**Altered granodiorite**	**Dolerite**	**Alt dolerite–granodiorite contact**	**Alt dolerite**	**Alt dolerite**
Sample analysed	**Least alt granodiorite**	**Qtz–carb vein ± sul**	**Sul vein and alt dolerite**	**Alt dolerite–granodiorite contact**	**Qtz–gal vein**	**Qtz–gal–cpy vein**
wt%						
SiO_2	67.25	76.73	na	65.07	na	na
Al_2O_3	15.32	10.81	na	13.29	na	na
Fe_2O_3(T)	4.82	3.43	na	8.76	na	na
MnO	0.08	0.11	na	0.10	na	na
MgO	1.88	0.97	na	2.44	na	na
CaO	0.93	0.13	na	1.45	na	na
Na_2O	5.03	1.31	na	4.36	na	na
K_2O	2.13	6.04	na	2.14	na	na
TiO_2	0.41	0.06	na	0.78	na	na
P_2O_5	0.16	0.02	na	0.54	na	na
LOI	1.07	1.16	na	1.34	na	na
Total	99.07	100.80	na	100.30	na	na
C-Total	0.02	0.23	na	0.05	na	na
S-Total	0.05	bdl	na	0.65	na	na
ppm						
Au	bdl	0.015	0.240	0.046	bdl	11.300
Ag	0.80	bdl	20.0	6.0	14.4	116.0
As	bdl	1.7	27.1	1.8	1.5	10.2
Sb	bdl	bdl	6.00	1.20	4.90	45.90
Hg	bdl	bdl	bdl	bdl	bdl	3.00
Te	bdl	bdl	bdl	bdl	na	na
Bi	0.09	0.03	1.44	0.14	na	na
Mo	1.4	0.7	bdl	0.8	bdl	bdl
Li	18.7	8.5	34.1	23.4	na	na
W	bdl	0.3	bdl	0.1	bdl	bdl
Sn	2	bdl	2	3	na	na
Cu	20	4	4710	120	304	10000
Pb	9.1	23	7100	65	6100	55000
Zn	90	40	320	120	169	8810
Cr	80	100	100	80	na	na
Ni	3	4	40	11	12	12
Co	8.5	6.1	42.9	16.4	na	na
V	74	15	618	80	na	na
Au/Ag	<0.01[a]	0.30	0.01	<0.01[a]	<0.01[a]	0.10
Au/Cu	<0.01[a]	<0.01[a]	<0.01[a]	<0.01[a]	<0.01[a]	<0.01[a]
As+Sb	0	2	33	3	6	56
Mo+Bi+W+Li	20	10	36	24	–	–
Sn+W	2	1	2	3	–	–
Cu+Pb+Zn	119	67	10030	305	5473	23810
Cs	1.66	1.01	0.69	3.33	na	na
Rb	66	57	27	112	na	na
Ba	511	1012	453	341	bdl	170
Sr	172	51	11	122	na	na
Th	16.2	2.5	1.4	32.6	na	na
U	4.6	1.0	1.5	4.5	na	na
Zr	148	88	149	817	na	na
Hf	3.2	0.2	1.2	0.2	na	na
Nb	17	3	10	28	na	na
Ta	1.6	0.3	1.0	1.4	na	na
Sc	13	2	48	13	na	na
Y	12	3	55	33	na	na
Se	bdl	bdl	5.1	1.1	na	na
Be	3.1	0.8	1.2	2.1	na	na
Cd	bdl	bdl	4.6	bdl	7.4	168
Ga	21.9	12.1	28.2	20.8	na	na
Ge	2	1	3	2	na	na
In	bdl	bdl	0.9	bdl	na	na
Re	0.002	0.001	0.003	0.004	na	na
Tl	0.24	0.18	0.12	0.5	na	na

Abbreviations: bdl, below detection limit; na, not analysed; Alt, altered; carb, carbonate; cpy, chalcopyrite; gal, galena; qtz, quartz; sul, sulfide.

Note: [a]Detection limit value use to calculated the ratio; –, not calculated.

with amphibolite bands and marble (Figure 15). These two stratigraphic groups are separated by a thrust fault trending N–S and dipping eastwards (Figure 15). The Karasuk Group has been thrusted over the Karamoja Group; rocks in both stratigraphic groups striking between N–S and N10°E, and displaying a vertical to subvertical dip (Baguma 2001). Rocks in the Karamoja area have been crosscut by a series of NE–SW- and E–W-trending subvertical faults that are locally occupied by dykes and pegmatites (Figure 15).

STRUCTURAL SETTING, REGIONAL METAMORPHISM AND ALTERATION

Sanders (1965) suggested that the Karamoja area consists of essentially an imbricate stack of thrust slices of the Archean basement with subordinate remnants of Proterozoic sedimentary rocks, mainly meta-arkose. These rocks strike northwards and are defined by N–S-trending thrusts (Figures 15, 16). Rocks in the Karamoja gold district display a strong, approximately N–S-striking,

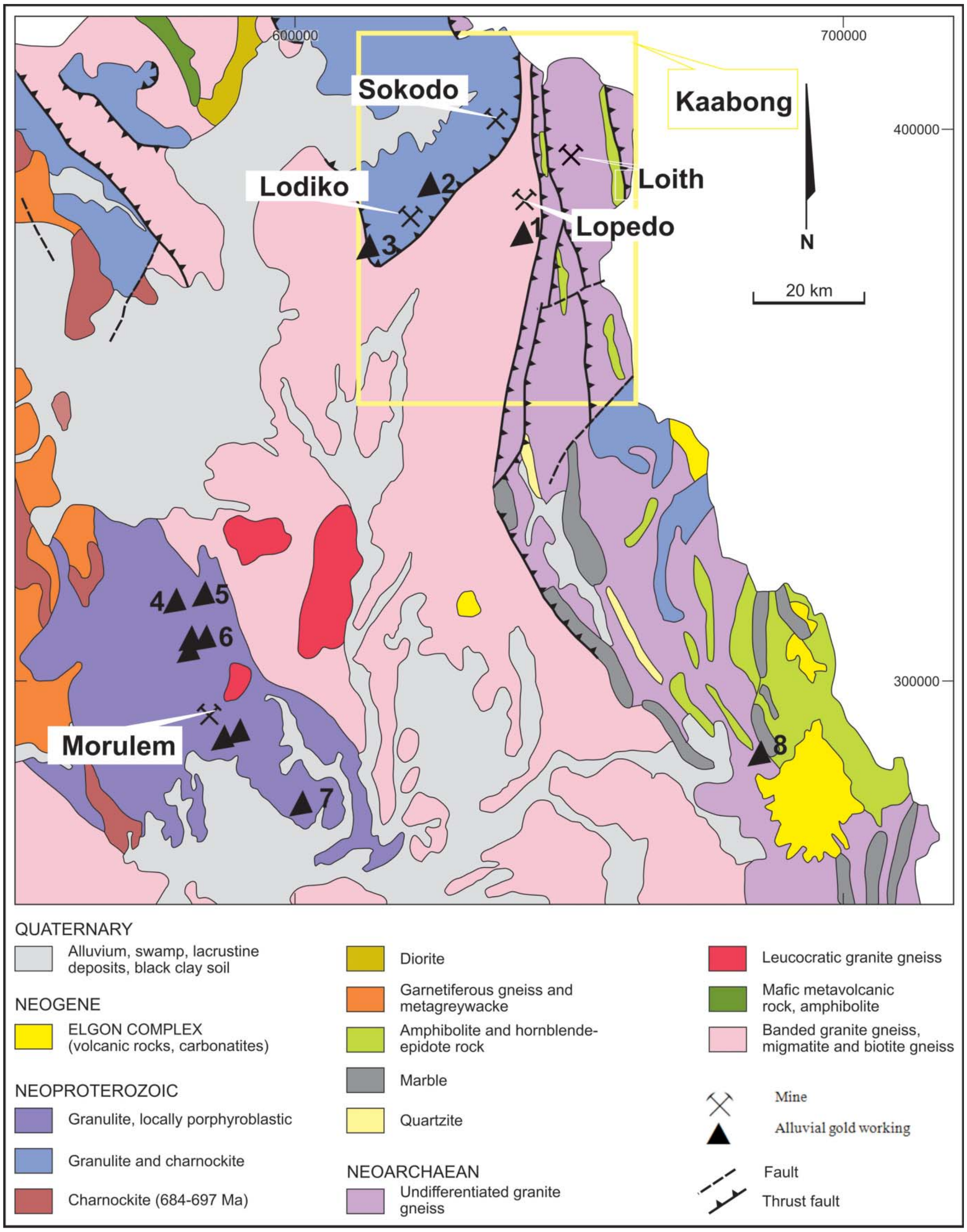

Figure 15 Geological map of the Karamoja gold district showing gold mines and alluvial workings (modified after Williams 1966; Baguma 2001; Baglow *et al.* 2012b). Alluvial workings: 1, Nakapel-Kekuil; 2, Nariobwol; 3, Kopoth; 4, Alerek; 5, Lokemer; 6, Angorom; 7, Rogomolim west; 8, Rupa.

subvertical to steeply E- and W-dipping foliation and metamorphic bands. The geometry of the foliation suggests tight to isoclinal folds, with a shallow NNW plunge (Baguma 2001). Faults are well developed in the northern part of the Karamoja area with a general ENE strike and dip of 75°NW. The fault zones are usually between 3 and 15 m wide, and in some places are filled by foliated granite dykes.

According to Tanner (1973), the metamorphism that affects supracrustal rocks within the Mozambique belt is typically Barrovian with the widespread development of garnet, kyanite and sillimanite. The metamorphic grade of the rocks in the Karamoja gold district is upper amphibolite to lower granulite facies. In the NW, granulite facies assemblages are characterised by hypersthene and diopside, and in places rocks are migmatised (Fleuty 1968). Locally, sillimanite–almandine assemblages constrain the metamorphic grade to upper amphibolite facies (Tuhumwrire 1991). According to MacGregor (1962), the Karamoja area contains rocks of the 'Basement Complex,' which is an assemblage of sedimentary rocks with minor igneous intrusions that have been intensely deformed, granitised and metamorphosed to amphibolites facies. The differences in metamorphic grade may be interpreted as simply varying metamorphic grade within one phase of regional metamorphism, or alternatively may suggest that the rocks in the NW belong to different tectonic groups that were emplaced via thrust faults (Fleuty 1968).

GOLD MINERALISATION

Gold in metasedimentary rocks within the Kaabong area (Figure 16), in the northern Karamoja gold district, was first reported by Biggs (1950). Since then, no detailed geoscientific investigations have been conducted in the area mainly due to poor accessibility, insecurity and the hostile nature of the Karamojong tribes settled in these areas. Branch Energy Uganda Limited carried out systematic regional stream sediment sampling programme between 1996 and 1998, but the results are presently inaccessible. According to Data *et al.* (2009), gold in the Karamoja gold district is located in lenticular bodies of quartz in N–S-trending shear zones, closely associated with the contact between granitic gneisses and metasedimentary rocks. Arsenopyrite is the typical ore mineral associated with gold. Gold in shallow open pits and in alluvial mines has been exploited in several locations (Figures 15, 16); production and grades have not been recorded.

LOPEDO GOLD MINE

The Lopedo gold mine, located in the Kaabong area within the NE corner of the Karamoja gold district (Figure 16), is characterised by a series of N–S-trending shear zones emplaced in Neoarchean granitic gneisses. The gold mine consists of a series of open pits with depths between 10 and 40 m, and lengths and widths of 10–300 m and 2–20 m, respectively (Figure 17A). Gold mineralisation is contained within quartz–microcline–plagioclase–biotite–hornblende veins and hydrothermally altered granite gneiss wallrock (Figure 17B). According to Baguma (2001), gold grades vary between 0.1 g/t and 10 g/t Au.

The hydrothermally altered granite gneiss is foliated, medium- to coarse-grained, granoblastic and locally porphyritic, and consists of quartz, microcline, plagioclase, biotite and muscovite (Figure 17A, B). The granite gneiss is highly migmatised showing both leuco- and melanosomes. Subhedral tabular biotite crystals are interlocked in quartz, microline and plagioclase grains, and have also been observed to overprint the main foliation fabric. Euhedral muscovite crystals overprint biotite and plagioclase and possibly post-date foliation (Figure 17C, F). Locally, anhedral to subhedral garnet grains overprint the main fabric. The altered gneiss contains small (<5 cm) veinlets, comprising quartz–microcline–plagioclase–biotite–hornblende and traces of garnets and apatite that pinch and swell with widths of 1–30 cm and are oriented subparallel to the N30°W-striking and 80°NE-dipping foliation. Hydrothermal biotite, muscovite and hornblende are the dominant mineral in these shear veins and occur as pervasive flakes overprinting the main foliation fabric (Figure 17D–F). Locally, subhedral apatite, anhedral garnet and cubic pyrite crystals overprint quartz and feldspar grains (Figure 17F).

Other gold occurrences in Uganda

There are several areas in Uganda where alluvial gold mining and/or significant soil/rock chip Au values have been reported, but no primary source has been detected or mine established. These areas have presently not been assigned to a gold district and are described here as areas where there is a potential for primary gold mineralisation. These areas are shown in Figure 4.

(1) The Kitgum area within the Aswa shear zone in northern Uganda is characterised by Neoarchean rocks with several interpreted second-order shear zones emanating from the first-order Asxa shear zone. According to Baglow *et al.* (2012a), gold soil and stream sediment anomalies, along an interpreted second-order shear zone, have the potential for gold mineralisation.

(2) The Western Nile area represents the western extremity of the Bomu-Kibalian shield of NE Congo and is characterised by Neoarchean and Mesoarchean rocks that comprise banded and migmatitic and granite gneisses, amphibolites and garnet-amphibolites that generally strike NW and dip 35°NE (Data *et al.* 2009). In 1930, the Nile-Congo Divine Exploration Company prospected for gold in the areas of Wana and Isi near Moyo, but no reports can be traced (Data *et al.* 2009). Alluvial gold was also reported in streams in Okoro County with Harris (1942) postulating that gold mineralisation is hosted in mainly undifferentiated felsic gneisses and granulite facies rocks, and locally in granite and schists, quartzites and marbles. In 1960, alluvial gold specks were panned from the Nyagak River valley (Otika 1960). A map by Barnes (1961) displays Au localities between Arua and Rhino Camp, and near Zeu. Recent work by GTK used airborne geophysics and soil and stream sediment analyses to concentrate investigations on chert and BIF outcrops in Paidha and known placer gold areas in the Zeu area, close to the border of DRC (GTK

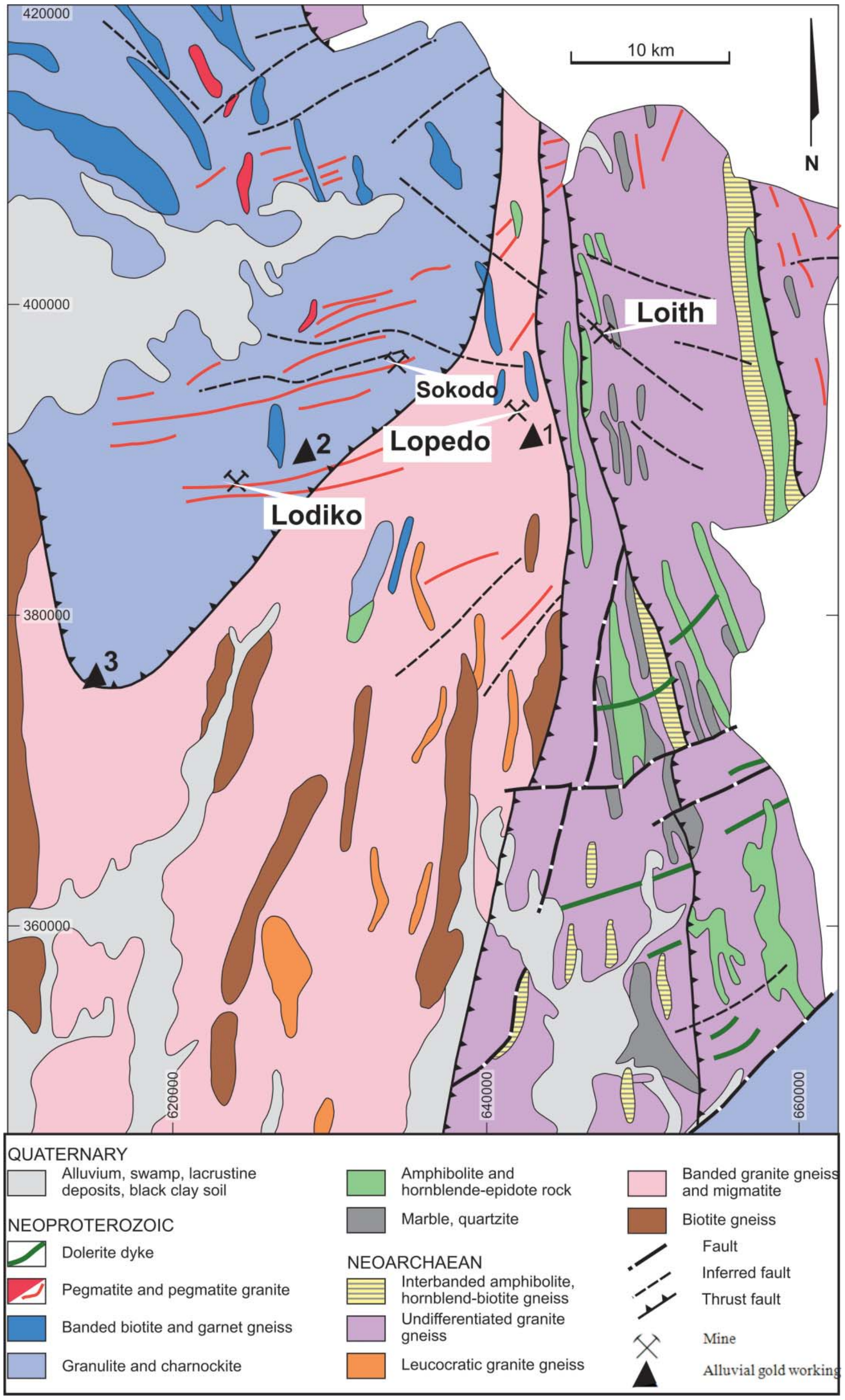

Figure 16 The geological map of the Kaabong area, northern Karamoja gold district (modified after Williams 1966; Baguma 2001; Baglow *et al.* 2012b). Alluvial gold workings: 1, Nakapel-Kekuil; 2, Nariobwol; 3, Kopoth.

Consortium 2012). The gold potential in the White Nile area has been largely inferred from the proximity of the Kilo-Moto greenstone belt and associated gold deposits (3 Mill oz Au produced; Westerhof 2012), which is located just S of the West Nile area in the DRC (Goossens 2009).

(3) Kabale-Kisoro area (Figure 18) is hosted in the Mesoproterozoic North Kibaran fold belt in SW Uganda (Figure 4). The North Kibaran belt is composed of folded and metamorphosed clastic sedimentary rocks, and pre- to synkinematic, foliated to isotropic porphyritic granite and pegmatite granite attributed to the North Kibaran Igneous Province (NKIP; Härmä *et al.* 2011). The NKIP manifests a period of accelerated extension during a relatively short interval between 1380 and 1375 Ma (Härmä *et al.* 2011). According to Tanner (1973) and Härmä *et al.* (2011), the mudstone–shale–phyllite succession in the Kabale-Kisoro area is characterised by regional-scale NW–SE-trending anticlines and synclines (Figure 18) metamorphosed to lower greenschist facies with regional development of chlorite and biotite. Alluvial gold workings in the Kabale-Kisoro area are displayed in Figure 18 (Data *et al.* 2009). Barnes (1961) reported gold nuggets, up to half an ounce in weight, with cassiterite, tungsten and bismuntite from Kiruruma in the central

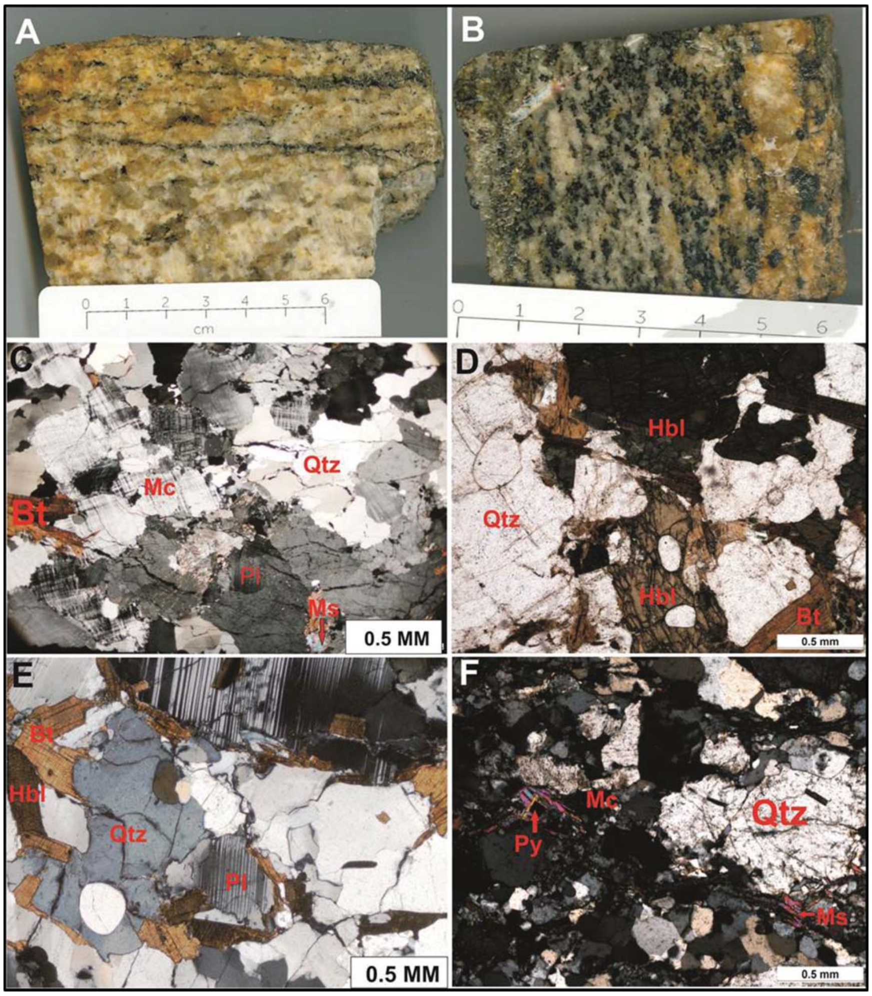

Figure 17 Photographs and photomicrographs of rock samples from the Lopedo mine. (A) Very coarse grained, granoblastic foliated granite gneiss, biotite overprints quartz–feldspar grains and forms thin (<1 mm) continuous bands along the foliation plane. (B) Medium-grained, thinly foliated and banded hornblende–biotite gneiss. (C) Mc-microcline–Qtz-quartz–Pl-plagioclase grain intergrowth overprinted by tabular Bt-biotite and Ms-muscovite grains in granite gneiss. (D) Intergrown Qtz-quartz–Mc-microcline grains overprinted by tabular Bt-biotite and Hbl-hornblende grains in altered gneiss. (E) Quartz–plagioclase ± microcline grain intergrowth overprinted by biotite–hornblende grains along grain margins in a biotite–hornblende gneiss. (F) Intergrown Mc-microcline–Qtz-quartz grains overprinted by tabular muscovite grains in altered gneiss, locally cubic Py-pyrite crystals.

part of the Kabale-Kisoro area. Based on the regional metallogeny and the presence of these minerals, the origin of gold is likely associated with Sn–W–Nb–Ta granites exploited in the area.

DISCUSSION

A close examination of the geological characteristics of the different gold districts in Uganda reveals many common geological features as well as significant differences between gold districts and mines at a variety of scales. The common features include: (1) strong structural control of the mineralised areas; (2) relatively late timing of gold mineralisation with respect to regional metamorphism and deformation; and (3) hydrothermal alteration associated and controlled by structures such as shear zones and associated vein/reef systems.

All mines described in this project display a structural control. For example, the Tira, Kamalenge and Kitaka mines are located in brittle-ductile shear zones, whereas the Muti, Lopedo mines and many other gold occurrences in the Kaabong area of the Karamoja gold district are located in ductile shear zones (Table 3). Quartz veins are characteristically emplaced subparallel to the shear zones, i.e. they represent shear veins (cf. Hodgson 1989). In all of these mines, the ore-hosting structures including quartz veins are undeformed, i.e. they were emplaced during the last deformation event in the area.

In all of the deposits described, hydrothermal minerals replace metamorphic minerals; for example, at the Tira deposits, carbonate and chlorite replace metamorphic amphiboles and plagioclase in metadolerite distal from the gold-bearing veins where the gold content of the hydrothermally altered rock is still low (<1 g/t Au). The disseminated pyrite and gold in the shear vein (reef) and the disseminated pyrite in the wallrock that immediately borders the reefs are all undeformed; sulfides display synkinematic textures with respect to the emplacement of the gold-bearing shear zones, but they have not been deformed themselves. At the Kitaka mine, massive galena with perfect cleavage and coarse crystalline chalcopyrite suggest their emplacement late in the formation of the shear zone and associated quartz vein system. Hydrothermal alteration minerals such as chlorite, carbonate and sericite replace the greenschist facies metamorphic minerals in the granodiorite and dolerite host rocks. At the Lopedo mine, high-temperature hydrothermal alteration minerals such as pyroxene, plagioclase and garnets are strongly foliated parallel to the ductile shear zones that contain the mineralised ore zone. Euhedral muscovite and garnet overprint the foliation,

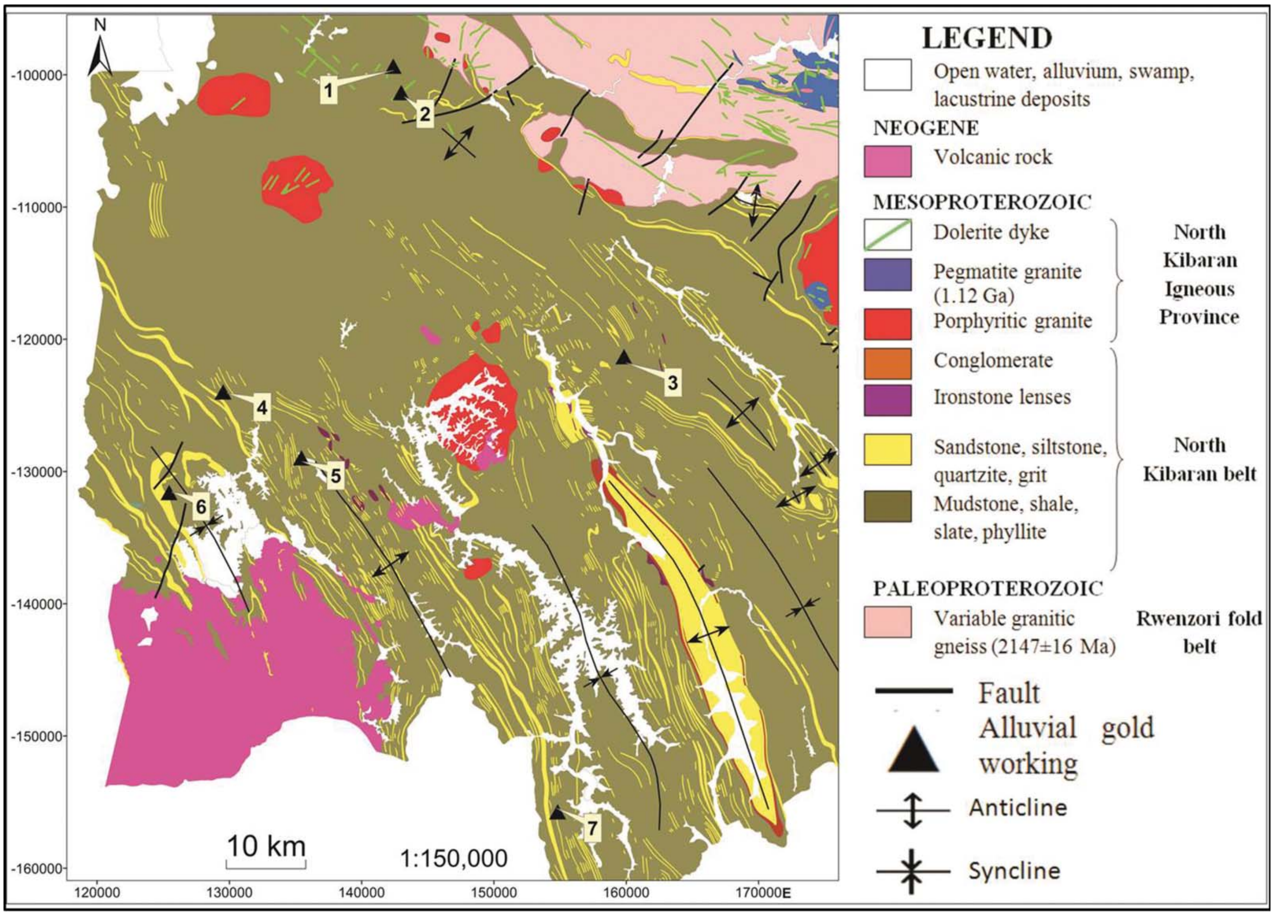

Figure 18 The geological map of the Kabale-Kisoro area (modified after Lindh *et al.* 2011; Manninen *et al.* 2011) displaying areas of alluvial gold workings: 1 Kanungu, 2 Kashenyi, 3 Kiruruma, 4 Rubuguri, 5 Mirindi, 6 Karamba, 7 Mugyera.

suggesting their late kinematic timing. Importantly, the shear zones and quartz–carbonate–plagioclase veinlets are not deformed. However, recent research on structurally controlled, high-temperature gold deposits such as at Griffins Find in Western Australia (Tomkins & Grundy 2009), Challenger in South Australia (Tomkins & Mavrogenes 2002) and Hemlo in Ontario, Canada (Lin 2001; Tomkins *et al.* 2004) have demonstrated that these deposits were emplaced prior to peak metamorphism and then subsequently metamorphosed, i.e. these deposits represent a metamorphosed gold system (Hagemann & Gilg 2011). At the Lopedo mine and other gold occurrences in the Karamoja gold district, the metamorphic grade of the host rocks is sufficiently high, i.e. lower granulite facies metamorphism, that this possibility has to be taken into account.

Hydrothermal alteration in all presently known gold deposits and mineralised areas in Uganda is spatially and geometrically controlled by structures such as brittle-ductile or ductile shear zones and associated vein systems (Table 3). For example, at the Tira mine, the geometry of the gold-rich zones is strongly controlled by the ductile shear zones that contain the quartz reefs. Away from these zones (e.g. 2 m) the gold values drop off markedly; further away (e.g. >20 m) the hydrothermal alteration minerals are absent; and the metadolerite consists of igneous and metamorphic minerals only. The same shear zone controlled alteration and mineralisation geometry can be observed at the Kitaka and Mashonga mines.

Features that are different between gold mines and districts are: (1) ages and tectonic setting of rocks in which gold mineralisation is emplaced, (2) host lithologies, (3) styles of mineralisation and ore mineralogy, and (4) hydrothermal alteration systematics.

Gold deposits in Uganda are hosted by a variety of host rocks and metamorphic grades and formed as part of orogenic activity from the Archean (e.g. the Busia gold district in the Busia-Kakamega greenstone belt) to the Paleoproterozoic (e.g. Mubende and Buhweju-Mashonga gold districts in the Rwenzori fold belt), the Mesoproterozoic (e.g. the Kabale-Kisoro area in the North Kibaran fold belt) and the Neoproterozoic (e.g. the Karamoja gold district in the Mozambique fold belt and Kitgum area; Table 3).

At the Tira mine, gold is hosted in dolerite, basalt and sedimentary rocks that are metamorphosed to lower greenschist facies. In contrast, in the Karamoja district, gold is hosted by lower granulite facies gneisses and amphibolites. Gold mineralisation in the Mubende, Buhweju and Mashonga gold districts is mainly hosted in sedimentary rocks including shales, siltstone, sandstone that are metamorphosed to lower greenschist facies. At the Kataka mine, a granodiorite, possibly part of a

Table 3 Key geological characteristics of gold mines in Uganda.

Gold district	Mine	Tectonic setting	Eras	Host rocks	Metarmorphic grade	Structural control	Mineralisation style	Alteration minerals	Ore assemblage
Busia	Tira	Busia-Kakamega greenstone belt	Neoarchean	Dolerite, basalt and sedimentary rocks	Lower greenschist facies	Brittle-ductile shear zones	Sul and gold in shear veins (reefs), crack-seal textured, laminated veins	Carbonate, chlorite, sericite	Pyrite–hematite ± chalcopyrite ± gold
Mubende	Kamalenge	Rwenzori fold belt	Paleoproterozoic	Sedimentary rocks including, e.g. shale, siltstone, sandstone	Lower greenschist facies	Brittle-ductile shear zones	Sul and gold in veins and subparallel to shear zones; sul diss in wallrocks	Sericite–chlorite	Pyrite–gold; hematite
Buhweju-Mashonga	Kitaka	Rwenzori fold belt	Paleoproterozoic	Granodiorite and dolerite	Greenschist facies	Brittle-ductile shear zones	Sul and gold in crack-seal textured, laminated veins	Chlorite, carbonate, sericite	Galena–chalcopyrite–pyrite ± chalcocite ± gold
Buhweju-Mashonga	Muti	Rwenzori fold belt	Paleoproterozoic	Sedimentary rocks including, e.g. shale, siltstone, sandstone	Lower greenschist facies	Ductile shear zones	Vein and disseminated sul and gold in wallrocks	Sericite	Pyrite–gold
Buhweju-Mashonga	Mashonga	Rwenzori fold belt	Paleoproterozoic	Sedimentary rocks including, e.g. shale, siltstone, sandstone	Lower greenschist facies	Ductile shear zones	Diss sul and gold in ductile shear zones or mylonite zones; diss sul and gold in wallrocks	Sericite, chlorite	Gold ± pyrite ± pyrrhotite
Buhweju-Mashonga	Kanywambogo	Rwenzori fold belt	Paleoproterozoic	Sedimentary rocks including, e.g. shales, siltstone, sandstone	Lower greenschist facies	Ductile shear zones	Diss sul and gold in shear veins, locally brecciated	Sericite	Galena–chalcopyrite–pyrite ± chalcocite ± gold
Karamoja	Lopedo	Mozambique fold belt	Neo-proterozoic	Gneiss and amphibolite	Lower granulite facies metamorphism	Ductile shear zones	Diss sul and gold in veins and veinlets in ductile shear zones; diss sul and gold in wallrocks	Pyroxene, biotite, sericite, hornblende, garnet	Pyrite ± gold

Abbreviations: sul, sulfide; diss, disseminated.

differentiated dolerite intrusion, hosts gold mineralisation. The variety of host rocks for gold mineralisation is similar to that encountered in other Archean cratons and Proterozoic belts such as in the Archean Abitibi greenstone belt in the Superior province of Canada (Poulsen *et al.* 2000), the Norseman-Wiluna belt in the Yilgarn craton of Western Australia (Hagemann & Cassidy 2000), the Proterozoic Paterson province in Western Australia (e.g. the siltstone–sandstone hosted Telfer deposit; Goellnicht *et al.* 1989; Rowins *et al.* 1997) and the Brasilia fold belt in Brazil (e.g. the phyllite hosted Morro de Ouro deposit; Freitas-Silva *et al.* 1991).

The styles of gold mineralisation and ore mineralogy are variable (Table 3) and include: (1) quartz–carbonate shear veins including quartz–carbonate reefs (i.e. veins with width >1 m) that contain pyrite–gold and 'free' gold and locally may be brecciated, e.g. the Tira and Kanywambogo mines; (2) crack-seal textured, laminated quartz–pyrite–gold veins, e.g. the Tira and Kitaka mines; (3) semimassive pyrite-rich wallrocks, with gold inclusions in pyrite, close to shear zones or veins, e.g. at the Tira mine; (4) disseminated sulfides and gold in the wallrocks adjacent to shear zones and/or veins, e.g. mines in the Karamoja gold district; and (5) ductile shear zones or mylonite zones with disseminated gold–pyrite–pyrrhotite, e.g. the Mashonga mine. All of these mineralisation styles have also been documented in gold deposits in Archean granite–greenstone belts and Proterozoic fold belts worldwide, including, for example, in Canada (Colvine *et al.* 1988), Western Australia (Groves *et al.* 1998), Brazil (Lobato *et al.* 2001) or western Africa (Oberthur *et al.* 1997).

The hydrothermal alteration minerals observed in the different deposits and districts are different with respect to the mineral species and assemblages but are broadly compatible in pressure–temperature with the metamorphic facies observed in the host rocks, which contain gold mineralisation. This suggests that there is a relative timing relationship between gold mineralisation and regional metamorphism, i.e. hydrothermal alteration is relatively late, either synchronous or post-peak metamorphism. This in turn also suggests that hydrothermal alteration and gold mineralisation are emplaced at distinct paleocrustal levels (cf. Colvine *et al.* 1988; Groves *et al.* 1998). At the Tira mine, carbonate and chlorite replace greenschist facies amphiboles and plagioclase, which, together with pyrite are in equilibrium with gold. Silicate–carbonate–sulfide–gold assemblages are compatible with a mesozonal, low- to mid-crustal level formation of the gold system (cf. Mueller & Groves 1991; Hagemann & Cassidy 2000). At the Kitaka and Mashonga mines, the same mid-crustal level, mesozonal hydrothermal alteration and mineralisation are deduced from the key alteration and ore minerals (Table 3). In the Karamoja gold district, observations in the field and petrography of hydrothermally altered rocks suggest that hydrothermal alteration minerals, such as pyroxene, plagioclase and garnets, replace the lower granulite facies metamorphic assemblages. This is compatible with a hypozonal, lower-crustal level of formation of these minerals. The location of Archean gold deposits at different structural levels and metamorphic terranes was first postulated by Colvine *et al.* (1988) for lode gold deposits in Ontario (Canada) and later refined by Groves *et al.* (1992) and Gebre-Mariam *et al.* (1995), who proposed a crustal continuum of gold deposits in the Archean granite–greenstone belts in Western Australia. The crustal-continuum model was later extended to Proterozoic and younger terranes (Goldfarb *et al.* 2001).

Most gold mines, for which public material is available and which have been described in this project, can be interpreted to belong to the 'orogenic gold deposit' class of Groves *et al.* (1998) or the 'orogenic gold system' of Hagemann & Cassidy (2000). Some of these, e.g. the Mashonga mine, may belong to the orogenic gold subclass of intrusion-related gold system given their close spatial relationship to granites observed <150 m from the mine. However, detailed geochronology of gold mineralisation and constraints on the ore fluid chemistry are necessary to establish the genetic link between gold mineralisation and magmatism. The mine least compatible with an orogenic gold system is the Kitaka mine, which has a very high base metal content, expressed by massive chalcopyrite and galena in the gold-bearing veins (Figure 13). Based on the high Cu content, in addition to gold, it may be related to the intrusion-related gold class (cf. Sillitoe 1991; Sillitoe & Thompson 1998). However, the high galena content, in addition to copper and gold, is rather unusual and is not compatible with this gold class. Furthermore, there are orogenic gold systems, e.g. the New Holland deposit near Leonora in Western Australia (Ackroyd *et al.* 2001), that display lodes with a significant amount of galena and chalcopyrite. Given the limited underground exposure and absence of diamond core at Kitaka, it is possible that at the presently exposed (and sampled) lode galena and sphalerite are predominant, but that over the entire mineralised area, base metals are only subordinate. Further mining and documentation of the ore mineralogy will hopefully assist in formulating a robust deposit model for the Kitaka mine.

As noted above, gold mineralisation in the northern Karamoja gold district, particularly those mines in the Kaabong area, which are hosted in high temperature ductile shear zones, may not have formed at hypozonal crustal levels synchronous with granulite facies metamorphism and emplacement of ductile shear zones but rather formed prior to metamorphism and were then subsequently metamorphosed, therefore belonging to the metamorphosed gold system. Examples for deposits that belong to this gold system include the Hemlo, Challenger and Griffins Find deposits (Tompkins & Grundy 2009; Hagemann & Gilg 2011).

The geochemical database on hydrothermally altered and mineralised rocks from gold deposits in Uganda is presently limited; therefore, interpretations have to be taken cautiously. The As–Sb enrichment in mineralised samples is typical for many metavolcanic and metasedimentary hosted gold deposits (Hagemann & Cassidy 2000). It is therefore surprising that the Tira mine displays only a moderate correlation of Au with As+Sb (Figure 9A). The felsic magma element signature of Mo+Bi+W+Li and reduced felsic magma element signature of Sn+W, which are normally more strongly developed in granite-hosted and/or granite-related gold deposits, display a positive correlation with Au at the

Tira mine (Figure 10C). This may suggest a magmatic contribution of the ore fluids and/or fluid–rock reactions between the ore fluids and the granites exposed in the Tira mine. Pathfinder elements in the Tira mine are closely linked to the distal hydrothermal alteration minerals carbonate, chlorite, sericite and sulfides. Therefore, any carbon, potassium, sulfur or iron enrichment in those metavolcanic rocks can be indicative (but not diagnostic) for Tira type mines in the Busia greenstone belt or other greenstone belts in Uganda. The geochemical dataset from the Kamalenge mine is limited, and the gold values are low; however, there is a positive correlation between Au and As and Sb, and a negative correlation between Au and the 'igneous' element association Mo+Bi+W+Li and base metals Cu+Pb+Zn. The high As and Sb signatures are likely a pathfinder element for gold in the Kamalenge area and possibly other metasedimentary Proterozoic fold belts in Uganda. They are compatible with orogenic gold systems hosted in metasedimentary rocks worldwide (Partington & Williams 2000).

The absence of other gold systems in Uganda such as gold-rich VHMS deposits (cf. Marquis *et al.* 1990; Yeats *et al.* 1996; Mercier-Langevin *et al.* 2007), gold-rich porphyries (Sillitoe 1997, 2000; Duuring *et al.* 2007), skarns (cf Mueller *et al.* 1996, 2008) or even epithermal-like deposits (Hagemann *et al.* 1994) is likely due to the lack of geological mapping and geochemical data and the lack of systematic exploration. Further detailed documentation of structures, hydrothermal alteration and the relationship between gold mineralisation and spatially and genetically related granitoids, is necessary to further constrain prospective areas for gold mineralisation in Uganda. In summary, the gold districts and mines in Uganda demonstrate a number of common features as well as a great diversity in a number of geological characteristics. The diversity of the mines reflects the complex interplay of physical and chemical processes at the trap site (deposit). These are localised at various paleocrustal levels, ranging from sub-greenschist to lower granulite facies metamorphic environments, with postulated gold precipitation over a correspondingly wide range of pressures and temperatures. The variability in depositional site characteristics largely reflects complex structural heterogeneities, the pressure–temperature conditions, proximity to syn-mineralisation granitoids, variability of host rock and local changes in ore-fluid composition.

CONCLUSIONS

This paper summarises all available geological information on gold mineralisation in Uganda and presents, for the first time, a coherent overview of the different gold districts and significant gold-rich areas. Interpretation of recently available geological mapping, geochronological data and constraints on the tectonic settings in Uganda, combined with petrographical and geochemical analyses of hydrothermally altered and mineralised rocks from different mines and districts and observations in the field by the authors, has revealed the following:

There are four recognised gold districts in Uganda: (1) the Busia gold district hosted in the Neoarchean Busia-Kakamega granite–greenstone belt in the SE of Uganda, which contains the structurally controlled mesozonal Tira gold mine; (2) the Mubende gold district in the Paleoproterozoic Rwenzori fold belt in central Uganda, which hosts the structurally controlled metasediment hosted mesozonal Kamalenge and Kisita gold mines; (3) the Buhweju-Mashonga gold district in SW Uganda, which contains the vein hosted Pb–Zn–Au Kitaka mine, the structurally controlled intrusion-hosted mesozonal Mashonga gold mine and the structurally controlled sandstone-hosted mesozonal Muti and Kanywambogo mines; and (4) the Karamoja gold district hosted either in reworked Archean basement rocks and/or in the upper amphibolite–lower granulite facies rocks of the Neoproterozoic Mozambique fold belt in NE and W Uganda. The northern part of the Karamoja gold district contains numerous hypozonal shear zone controlled gold mines. Other areas in Uganda where alluvial gold and/or shallow gold workings are reported include the Kitgum area within the Aswa shear zone in northern Uganda, the Western Nile area, which represents the western extremity of the Bomu-Kibalian shield of NE Congo, and the Kabale-Kisoro area located in the Mesoproterozoic North Kibaran fold belt in SW Uganda.

Preliminary analyses of geological features of gold mineralisation in mines and districts suggest that the majority of those belong to the orogenic gold system (cf. Hagemann & Cassidy 2000). This is largely based on common geological features including: (1) strong structural control of mineralised areas through shear zones and associated quartz veins systems; (2) relative late timing of gold mineralisation with respect to regional greenschist–amphibolite facies metamorphism and deformation; and (3) hydrothermal alteration associated and controlled by structures such as shear zones and associated vein/reef system. Geological features that are different between gold mines and districts, but still compatible with the orogenic gold system, include: (1) the age and tectonic setting of rocks in which gold mineralisation is emplaced, ranging from the Archean to Neoproterozoic; (2) host lithologies ranging from metavolcanic to metasedimentray rocks; (3) styles of mineralisation and ore mineralogy including, e.g. vein hosted, disseminated shear zone hosted mineralisation; and (4) hydrothermal alteration systematics, which suggests that gold mineralisation was formed at different crustal levels.

Gold mineralisation at the Kitaka mine contains significant amounts of base metals, expressed by galena and chalcopyrite, which, if shown to be distributed over the entire mineralised area, is not compatible with an orogenic gold system. Mines in the Karamoja gold district may not belong to the hypozonal end-member of an orogenic gold system but rather represent a metamorphosed gold system. More detailed work on all aspects of gold mineralisation in these mines and districts needs to be conducted in order to provide more robust genetic models.

There is significant potential for undiscovered orogenic gold systems, including intrusion-hosted gold systems in all Archean granite–greenstone belts, including

Busia and the Western Nile area of the Congo craton. In addition, metasediment-hosted orogenic gold systems, particularly in Paleoproterozoic mobile belts such as the Rwenzori fold belt, are also very prospective. There is also potential presently undetected, intrusion-related gold systems in these fold belts.

The results of this study are a first attempt to systematically describe the lithostratigraphy, structure, hydrothermal alteration and ore mineralogy of known gold mines and occurrences of Uganda. Future studies, including geological mapping at all scales, emphasising the structural control of mineralisation, geochronology of both the host rocks to mineralisation and alteration minerals in equilibrium with gold, whole-rock, trace-element and REE geochemistry and mineralogical studies of hydrothermally altered and mineralised samples, will assist greatly in clarifying the distribution and origin of diverse gold systems in this presently poorly understood part of Africa.

ACKNOWLEDGEMENTS

We acknowledge the support and help of the Centre for Exploration Targeting (CET) research team especially my colleagues Dr Thomas Angerer, Dr Paul Duuring, Christian Schindler and Ana-Sophie Hensler for their friendly and professional support towards the success of this study. This project was initiated by the Geological Survey of Uganda and the Centre for Exploration Targeting, and was sponsored by Nero Resources Australia Pty and the Society for Economic Geology student chapter.

REFERENCES

Ackroyd B. J., Hagemann S. G., Neumayr P., Ingle L. J., Inwood N. A. & Smolonogov S. 2001. Hydrothermal alteration and gold mineralization at the sandstone-hosted New Holland gold deposit, Agnew-Lawlers gold camp, Western Australia. *In:* Hagemann S. G., Neumayr P. & Witt W. eds. *Gold camps in the Norseman-Wiluna belt, Yilgarn Craton, Western Australia*, pp. 99–126. Geological Survey of Western Australia.

Backman B., Salminen R., Elsenbroek J., Savolainen H. & Korkiakoski E. 2011. *Report of the geochemical surveys at Bombo target; geological mapping, geochemical surveys and mineral resources assessment in selected areas of Uganda*, Department of Geological Survey and Mines, Uganda.

Baglow N., Boger S., Elepu D., Härmä P., Jenett T., Koistinen T., Kuivasaari T., Kyagulanyi D., Kärkkäinen N., Lehtonen M. I., Manninen T., Mäkitie H., Pokki J., Schumann A., Staudt M. & Virransalo P. 2011. *Explanation of the Geology of Sheet SA-36-1 (Mbarara) 1:250,000*, Department of Geological Survey and Mines, Uganda.

Baglow N., Elepu D., Härmä P., De Kock G. S., Koistinen T., Kuivasaari T., Kärkkäinen N., Lehtonen M. I., Manninen T., Marimira E., Mäkitie H., Nyakecho C., Saalmann K., Virransalo P. & Staudt M. 2012a. *Explanation of the Geology of Sheets NA-36-2 and NA-36-6 (Kitgum and Gulu) 1:250,000*, Department of Geological Survey and Mines, Uganda.

Baglow N., Elepu D., Koistinen T., Kuivasaari T., Kärkkäinen N., Lehtonen M. I., Manninen T., Marimira E., Mäkitie H., Nyakecho C., Saalmann K., Virransalo P. & Staudt M. 2012b. *Explanation of the Geology of Sheets NB-36-15, NA-36-3, -4, -7 and -8 (Didinga, Kaabong, Lodwar, Aloi and Moroto) 1:250,000*, Department of Geological Survey and Mines, Uganda.

Baguma Z. M. A. 1991. *A report on pitting, logging, sampling and evaluation of Kamalenge Mine*. Department of Geological Survey and Mines, Uganda. BZ/8.

Baguma Z. M. A. 2001. *Mineral potential mapping for gold in the Kaabong area, Uganda, using GIS*, International Instituite for Aerospace Survey and Earth Sciences Enschede, The Netherlands.

Bahiru E. A. 2011. *Inter-relationship between lithology and structure and its control on gold in Buhweju area, SW of Uganda*, University of Twente, pp. 76.

Barnes J. W. 1961. *The Mineral Resources of Uganda*. Department of Geological Survey and Mines, Uganda, Bulletin No. 4.

Bonifacel N. & Mruma A. H. 2012. *Structural analysis, metamorphism, and geochemistry of the Archaean granitoids-greenstones of the Sukumaland Greenstone Belt around Geita Hills, Northern Tanzania*, Department of Geology, University of Dar es Salaam, Dar es Salaam, Tanzania.

Begg G. C., Griffin W. L., Natapov L. M., O'Reilly S. Y., Grand S. P., O'Neill C. J., Hronsky J. M. A., Djomani Y. P., Swain C. J., Deen T. & Bowden P. 2009. The lithospheric architecture of Africa: Seismic tomography, mantle petrology, and tectonic evolution. *Geosphere* **5**, 23–50.

Biggs E. E. 1950. *Prospecting in the Kalapata area, Karamoja. Department of Geological Survey and Mines, Uganda unpub.* Report No. EB/2.

Borg G. & Shackleton R. M. 1997. The Tanzania and NE Zaire Cratons. *In:* de Wit M. J. & Ashwal L. D. eds. *Greenstone Belts*, pp. 608–619. Clarendon Press, Oxford.

Cahen L. & Snelling N. J. 1984. *The geochronology and evolution of Africa*, Clarendon Press, Oxford.

Carr J. 2002. *Report/ work plan for the year 2002, Kisiita Mining Co. Ltd*, Department of Geological Survey and Mines, Uganda.

Colvine A. C., Fyon J. A., Heather K. B., Marmont S., Smith P. M. & Troop D. G. 1988. *Archean lode gold deposits in Ontario*. Mines and Minerals Division, Ontario Geological Survey, Miscellaneous Paper 139, 136 p.

Combe A. D. 1932. *The geology of South-West Ankole and adjacent territories with special reference to the tin deposits*, Department of Geological Survey and Mines, Uganda.

Combe A. D. 1933. *Buhweju mountains and part of the adjacent country.* Department of Geological Survey and Mines, Uganda. annual report, 1933, 23–26.

Combe A. D. 1939. *Geology of the Lubare area (western Ankole)*. Department of Geological Survey and Mines, Uganda, *Bulletin* **3**, 1–22.

Cratchley C. R. & Evans R. B. 1967. *Geophysical Surveys for mineral deposits in area C'D, Western Uganda*, Department of Geological Survey and Mines, Uganda.

Cutten H., Fernandez-Alonso M., de Waele B. & Tack L. 2004. *Age constraints for basin evolution and sedimentation in the "Northeastern Kibaran Belt": Orleans, Abstracts, 20th Colloquium African Geology (CAG20)*, p. 123.

Data G., Olarka P. & Nyakecho C. 2009. *Gold Prospects in Uganda: Metallic Mineral Fact Sheets*, Department of Geological and Mines, Uganda.

Davis K. A. 1934. *Geological map of parts of Samia (Budama) and Bukoli (Busoga), Eastern Province Uganda*, Department of Geological Survey and Mines, Uganda.

Davis K. A. 1956. *The geology of SE Uganda*. Department of Geological Survey and Mines, Uganda, Memoir No. 8, 77 p.

De Kock G. S., Koistinen T., Kuivasaari T., Kärkkäinen N., Lehtonen M. I., Manninen T., Mäkitie H. & Staudt M. 2012. *Explanation of the Geology of Sheets NA-36-1 and NA-36-5 (Arua and Pakwach) 1:250,000*, Department of Geological Survey and Mines, Uganda.

Duuring P., Cassidy K. F. & Hagemann S. G. 2007. Granitoid-associated orogenic, intrusion-related, and porphyry style metal deposits in the Archean Yilgarn craton, Western Australia. *Ore Geology Reviews* **32**, 157–186.

Elepu D., Grantham G., Härmä P., Jenett T., Koistinen T., Kuivasaari T., Kyagulanyi D., Kärkkäinen N., Lehtonen M. I., Manninen T., Mäkitie H., Schumann A. & Staudt M. 2011a. *Explanation of the Geology of Sheets NA-36-15 and SA-36-3 (Jinja and Homa Bay) 1:250,000*, Department of Geological Survey and Mines, Uganda.

Elepu D., Grantham G., Härmä P., Jenett T., de Kock G. S., Koistinen T., Kuivasaari T., Kyagulanyi D., Kärkkäinen N., Lehtonen M. I., Manninen T., Mäkitie H., Saalmann K., Schumann A. & Staudt M. 2011b. *Explanation of the Geology of Sheets NA-36-14 (Kampala) 1:250,000*, Department of Geological Survey and Mines, Uganda.

Elepu D., Härmä P., de Kock G. S., Koistinen T., Kuivasaari T., Kyagulanyi D., Kärkkäinen N., Lehtonen M. I., Manninen T., Mäkitie H., Saalmann

K. & Staudt M. 2012. *Explanation of the Geology of Sheets NA-36-11 and NA-36-12 (Mbale and Kapenguria) 1:250,000*, Department of Geological Survey and MInes, Uganda.

Fleuty M. J. 1968. *Explanation of the Geology of Sheet 27 (Moroto)*. Department of Geological Survey and Mines, Uganda. Report No. 13, pp. 65.

Freitas-Silva F. H., Dardenne M. A. & Jost H. 1991. Lithostructural control of the Morro do Ouro gold deposit, Paracatu, Minas Gerais. *In:* Ladeira E. A. ed. *Brazil Gold '91*, pp. 681–683. Balkeema.

Gabert G. 1990. Lithostratigraphic and tectonic setting of gold mineralisation in the Archaean cratons of Tanzania and Uganda, East Africa. *Precambrian Research* **46**, 59–69.

Gebre-Mariam M., Hagemann S. G. & Groves D. I. 1995. A classification scheme for epigenetic Archean lode-gold deposits. *Mineralium Deposita* **30**, 408–410.

Goellnicht N. M., Groves D. I., McNaughton N. J. & Dimo G. 1989. An epigenetic origin for the Telfer gold deposit, Western Australia. *In:* Keays R. R., Ramsay W. R. H. & Groves D. I. eds. *Economic Geology Monograph*, **6**, 151–167.

Goldfarb R. J., Groves D. I. & Gardoll S. 2001. Orogenic gold and geological time: A global synthesis. *Ore Geology Reviews* **18**, 1–75.

Goldfarb R. J., Baker T., Dubé B., Groves D. I., Hart C. J. R. & Gosselin P. 2005. Distribution, character, and genesis of gold deposits in metamorphic terranes. *Economic Geology 100th Anniversary volume* 407–450.

Goossens P. J. 2009. Mineral potential of the Democratic Republic of Congo: a geological scandal. *SEG Newsletter* **77**, 13–16.

Groves D. I., Barley M. E., Barnicoat A. C., Cassidy K. C., Fare R. J., Hagemann S. G., Ho S. E., Hronsky J. M. A., Mikucki E. J., Mueller A. G., McNaughton N. J., Perring C. S., Ridley J. R. & Vearncombe J. R. 1992. Sub-greenschist- to granulite-hosted Archaean lode-gold deposits of the Yilgarn Craton: a depositional continuum from deep-sourced hydrothermal fluids in crustal-scale plumbing systems. *In:* Glover J. E. & Ho S. E. eds. *Third International Archaean Symposium, Perth 1990, Proceedings Volume*, p. 325–338. Nedlands, University of Western Australia Geology Department University Extension Publication 22.

Groves D. I., Condie K. C., Goldfarb R. J., Hronsky J. M. A. & Vielreicher R. M. 2005. Secular changes in global tectonic processes and their influence on the temporal distribution of gold-bearing mineral deposits. *Economic Geology* **100**, 203–224.

Groves D. I., Goldfarb R. J., Gebre-Mariam M., Hagemann S. G. & Robert F. 1998. Orogenic gold deposits: A proposed classification in the context of their crustal distribution and relationship to other gold deposit types. *Ore Geology Reviews* **13**, 7–27.

Groves D. I., Goldfarb R. J., Robert F. & Hart C. J. R. 2003. Gold deposits in metamorphic belts: overview of current understanding, outstanding problems, future research, and exploration significance. *Economic Geology* **98**, 1–29.

GTK Consortium 2012. *New potential targets for mineral exploration; geological mapping, geochemical surveys and mineral resources assessment in selected areas of Uganda*, Department of Geological Survey and Mines, Uganda.

Hagemann S. G. & Cassidy K. F. 2000. Archean orogenic lode gold deposits. *In:* Hagemann S. G. & Brown P. E. eds. *Gold in 2000*, pp. 9–68, SEG Reviews 13.

Hagemann S. G. & Gilg H. A. 2011. Oxygen and hydrogen isotope study of the Achaean granulite-hosted Griffin's Find gold deposit, Western Australia. *In:* Reich M., Barra F. & Tornos F. eds. *Proceedings of the 11th Biennial Meeting of the Society for Geology Applied to Mineral Deposits*, pp. 557–559. SGA, Antofagasta, Chile, 26–29th September 2011.

Hagemann S. G., Gebre-Mariam M. & Groves D. I. 1994. Surface water influx in shallow-level Archean lode-gold deposits in Western Australia. *Geology* **22**, 1067–1070.

Härmä P., Elepu D., Koistinen T., Kuivasaari T., Kärkkäinen N., Lehtonen M. I., Manninen T., Mäkitie H., Pokki J., Saalmann K., Staudt M. & Virransalo P. 2011. *Explanation of the Geology of Sheets NA-36-5 (Kabale) 1:250,000*, Department of Geological Survey and Mines, Uganda.

Harris N. 1942. *Interim report on the Petrography of part of West Nile district*. Department of Geological Survey and Mines, Uganda. Report No. NH/1.

Harris J. F. 1961. *Summary of the geology of Tanganyika; part IV: economic geology.* Geological Survey of Tanganyika, Memoir No. 1, Dar-es-Salaam, pp. 143.

Hepworth J. V. & Macdonald R. 1966. Orogenic Belts of the Northern Uganda Basement. *Nature* **210**, 726–727.

Hester B. W. 2009. *Gold exploration projects of Grey Crown Resources Limited Tira Gold Mine, Busia District*. Department of Geological Survey and Mines, Uganda.

Hodgson C. J. 1989. The structure of shear-related, vein-type gold deposits: A review. *Ore Geology Reviews* **4**, 231–273.

Ibrahim K. 2010. *Uganda begins refining gold domestically and from Congo*, The New Vision Uganda.

Johnson R. J. & Williams C. E. F. 1961. *Explanation of the Geology of Sheet 59 (Kiboga)*. Department of Geological Survey and Mines, Uganda. Report No. 7, pp. 39.

Kerrich R., Goldfarb R., Groves D. I. & Garwin S. 2000. Geodynamics of World-class gold deposits: Characteristics, space–time distributions and origins. Reviews in Economic Geology **13**, 501–551.

King B. C. 1941. *Report on W. Buckleys area, Kanyanseko, near Ruhoko, Kitoma, Ankole*. Department of geological Survey and Mines, Uganda. report, No. BCK/9.

Lehto T., Pekkala Y., Kuivasaari T., Kärkkäinen N., Konnunaho J., Ruotoistenmäki T., Turunen P. & Salminen R. 2011. *Provisional explorational programme for short, medium and long term; geological mapping, geochemical surveys and mineral resources assessment in selected areas of Uganda*, Department of Geological Survey and Mines.

Lin S. 2001. Stratigraphic and structural setting of the Hemlo gold deposit, Ontario, Canada. *Ecomic Geology* **96**, 477–507.

Lindh A., Janhila M. & Kuosmanen E. 2011. *Geological Map of Uganda, 1:500,000, Mineral potential areas (Draft), Uganda South of 1°; geological mapping, geochemical surveys and mineral resources assessment in selected areas of Uganda*, Department of Geological Survey and Mines, Uganda.

Lobato L. M., Ribeiro-Rodgrgues L. C. & Vieira F. W. R. 2001. Brazil's premier gold province. Part II: geology and genesis of gold deposits in the Archean Rio das Velhas greenstone belt, Quadrilatero Ferrifero. *Mineralium Deposita* **36**, 249–277.

Lytham J. D. 1965. *Kayonza area prospecting Report*. Department of Geological Survey and Mines, Uganda. unpublished Report No. JDL/1.

Lytham J. D. 1967. *Stream sediment Survey Impenetrable Forest Kigezi*. Department of Geological Survey and Mines, Uganda. unpublished Report No. JDL/5.

Macdonald R. 1961. *Explanation of the Geology of Sheet 36 (Nabilatuk) 1:100,000*. Department of Geological Survey and Mines, Uganda. Report No. 6, pp. 57.

Macdonald R. 1963. *Exploration of the Geology of Sheets 11 and 12 (Arua)*. Department of Geological Survey and Mines, Uganda. Report No. RM/46.

Macdonald R. 1966. *The Geology Atlas of Uganda*, Department of Geological Survey and Mines, Uganda.

MacGregor J. P. 1962. *Explanation of the Geology of Sheet 10 (Kaabong) 1:100,000*. Department of Geological Survey and Mines, Uganda. Report No. 9, pp. 42.

Mäkitie H., Baglow N., Boger S., Data G., de Kock G., Elepu D., Härmä P., Jenett T., Koistinen T., Kyagulanyi D., Lehtonen M. I., Manninen T., Mänttäri I., Pokki J., Schumann A., Westerhof A. B. & Virransalo P. 2011a. Giant c. 1.37 Ga arcuate dolerite dyke swarm in SW Uganda. *23rd Colloquium of African Geology, Abstract Volume* **256**, 8−14 January 2011, Johannesburg, South Africa.

Mäkitie H., Manninen T., Pokki J., Virransalo P., Jenett T., Boger S., Schumann A., Lehtonen M. I., Koistinen T., Lindh A., Janhila M. & Kuosmanen E. 2011b. *Geological map of Uganda, mineral potential areas, Kampala Sheet (NA-36-14) 1:250,000*, Department of Geological Survey and Mines, Uganda.

Manninen T., Mäkitie H., Pokki J., Virransalo P., Lehtonen M. I. & Koistinen T. 2011. *Geological map of Uganda, mineral potential areas, Kabale Sheet (NA-36-5) 1:250000*, Department of Geological Survey and Mines, Uganda.

Mänttäri I. 2009. *Radiometric ages for rock samples from Uganda; geological mapping, geochemical surveys and mineral resources assessment in selected areas of Uganda, GTK Consortium*. Department of Geological Survey and Mines, Uganda. Report 2, pp. 39, 1 App.

Mänttäri I. 2010a. *Radiometric ages for rock samples from Uganda; geological mapping, geochemical surveys and mineral resources assessment in selected areas of Uganda, GTK Consortium*. Department of Geological Survey and Mines, Uganda. Report 3, 2010.

Mänttäri I. I. 2010b. *Radiometric ages for rock samples from Uganda; geological mapping, geochemical surveys and mineral resources assessment in selected areas of Uganda, GTK Consortium*. Department of Geological Survey and Mines, Uganda. Report 4, 2010.

Mänttäri I. 2011. *Radiomentric ages for rock samples from Uganda, summary report for NDF project; geological mapping, geochemical surveys and mineral resources assessment in selected areas of Uganda, GTK Consortium*. Department of Geological Survey and Mines, Uganda.

Marquis P., Hubert C., Brown A. C. & Rigg D. M. 1990. Overprinting of early, redistributed Fe and Pb–Zn mineralization by late-stage Au–Ag–Cu deposition at the Dumagami mine, Bousquet district, Abitibi, Quebec. *Canadian Journal of Earth Sciences* **27**, 1651–1671.

Mercier-Langevin P., Dube B., Lafrance B., Hannington M., Galley A., Moorhead J. & Gosselin P. 2007. Metallogeny of the Doyon-Bousquet-LaRonde mining camp, Abitibi Greenstone Belt, Quebec. *In:* Goodfellow W. D. ed. *Mineral Deposits of Canada: A Synthesis of Major Deposit-Types, District Metallogeny, the Evolution of Geological Provinces, and Exploration Methods*, pp. 673–701. Geological Association of Canada, Mineral Deposits Division, Special Publication 5.

Mueller A. G. & Groves D. I. 1991. The classification of Western Australian greenstone-hosted gold deposits according to wallrock alteration mineral assemblages. *Ore Geology Reviews* **6**, 291–331.

Mueller A. G., Campbell I. H., Schiøtte L., Sevigny J. H. & Layer P. W. 1996. Constraints on the age of granitoid emplacement, metamorphism, gold mineralization, and subsequent cooling of the Archean greenstone terrane at Big Bell, Western Australia. *Economic Geology* **91**, 896–915.

Mueller A. G., Hall G. C., Nemchin A. A., Stein H. J., Creaser R. A. & Mason D. R. 2008. Archean high-Mg monzodiorite-syenite, epidote skarn, and biotite-sericite gold lodes in the Granny Smith-Wallaby district, Australia: U–Pb and Re–Os chronometry of two intrusion-related hydrothermal systems. *Mineralium Deposita* **43**, 337–362.

Nagudi B., Koeberl C. & Kurat G. 2003. Petrography and geochemistry of the Singo granite, Uganda, and implications for its origin. *Journal of African Earth Sciences* **36**, 73–87.

Oberthur T., Weiser T., Amanor J. A. & Chryssoulis S. I. 1997. Mineralogical siting and distribution of gold in quartz veins and sulphide ores of the Ashanti mine and other deposits in the Ashanti belt of Ghana: Genetic implications. *Mineralium Deposita* **32**, 2–15.

Old R. A. 1968. The geology of part of South-East Uganda. PhD thesis, Research Institute of African Geology, Leeds University, pp. 138.

Otika A. G. 1960. *Gold Prospecting in Nyagak Valley, West Nile*. Department of Geological Survey and Mines, Uganda. Report No. AGO/2.

Partington G. A. & Williams P. 2000. Proterozoic lode gold and (iron) copper–gold deposits: a comparison of Australian and global examples. *In*: Hagemann S. G. & Brown P. E. eds. *Gold in 2000*, pp. 69–101. SEG Reviews 13.

Pekkala Y., Baguma Z., Byamugisha S. & Turyasingura P. 1995. *Geochemical exploration programme on Gold and Base Metals, Buhweju, SW-Uganda. UNDP Project UGA/89/001*, Department of Geological Survey and Mines, Uganda.

Poulsen K. H., Robert F. & Dube B. 2000. Geological classification of Canadian gold deposits. *Geological Survey of Canada, Bulletin* **540**, 106.

Reece A. W. 1961. *Explanation of the Geology of Sheet 76 (Buhweju)*, Department of Geological Survey and Mines, Uganda.

Roberts R. O. 1940. *Notes on the geology of the gold–quartz vein occurrence at Mbogo mines near the Kanywambogo gold workings*. Department of Geological Survey and Mines, Uganda.

Rowins S. M., Groves D. I., McNaughton N. J., Palmer M. R. & Eldridge C. S. 1997. A reinterpretation of the role of granitoids in the genesis of Neoproterozoic gold mineralization in the Telfer Dome, Western Australia. *Economic Geology* **92**, 133–160.

Salminen R., Eklund M., Elsenbroek J., Savolainen H. & Korkiakoski E. 2011. *Report of the geochemical surveys at Buhweju target; geological mapping, geochemical surveys and mineral resources assessment in selected areas of Uganda, GTK Consortium*. Department of Geological Survey and Mines, Uganda.

Sanders L. D. 1965. Geology of the contact between the Nyanzian Shield and the Mozambique Belt in western Kenya. *Geological Survey Kenya, Report* **7**, 45.

Schlüter T. & Hampton C. 1997. *Geology of East Africa*, Gebruder Borntraeger, Berlin.

Schumann A. 2007. *Summary of the geology of the Tira area, its gold, and current and future exploration targets with a note on recent exploration results from MacAllister`s reef on EL 0030*, Busitema Mining Cie Ltd.

Sillitoe R. H. 1991. Intrusion-related gold deposits. *In*: Foster R. P. ed. *Gold Metallogeny and Exploration*, pp. 165–209. Blackie and Son, Glasgow.

Sillitoe R. H. 1997. Characteristics and controls of the largest porphyry copper–gold and epithermal gold deposits in the circum-Pacific region. *Australian Journal of Earth Sciences* **44**, 373–388.

Sillitoe R. H. 2000. Gold-rich porphyry deposits: descriptive and genetic models and their role in exploration and discovery. *In*: Hagemann S. G. & Brown P. E. eds. *Gold in 2000*, pp. 315–345. *SEG Reviews* **13**.

Sillitoe R. H. & Thompson J. F. H. 1998. Intrusion-related vein gold deposits: Types, tectono-magmatic settings, and difficulties of distinction from orogenic gold deposits. *Resource Geology* **48**, 237–250.

Simmons W. C. 1936. *Annual report for 1935*, Department of Geological Survey and Mines, Uganda.

Stern R. J. 1994. Arc assembly and continental collision in the Neoproterozoic East African Orogen: Implication for the consolidation of Gondwanaland. *Annual Reviews Earth and Planetary Science* **22**, 319−351.

Tack L., Duchesne J.-C., Liégeois J.-P. & Deblond A. 1994. Kibaran A-type granitoids and mafic rocks generated by two mantle sources in a late orogenic setting (Burundi). *Precambrian Research* **68**, 323−356.

Tack L., Wingate M. T. D., Waele B. D., Meert J., Griffin B., Belousova E. A., Tahon A., Fernandez-Alonso M., Baudet D., Cutten H. N. C. & Dewaele S. 2009. The Mesoproterozoic "Kibaran Event" in Central Africa: a 1375 Ma intracratonic emplacement of a Large Igneous Province (LIP). *Geological Society London*, Fermor Meeting "Rodinia: Supercontinents, superplumes and Scotland", Edinburgh, 9−13 September 2009.

Tanner P. W. G. 1973. Orogenic Cycles in East Africa. *Geological Society of America Bulletin* **84**, 2839–2850.

Tomkins A. G. & Grundy C. 2009. Upper temperature limits of orogenic gold deposit formation: constraints from the granulite-hosted Griffin's Find Deposit, Yilgarn Craton. *Economic Geology* **104**, p. 669–685.

Tomkins A. G. & Mavrogenes J. A. 2002. Mobilization of gold as a polymetallic melt during pelite anatexis at the Challenger deposit, South Australia: A metamorphosed Archaean gold deposit. *Economic Geology* **97**, 1249–1271.

Tomkins A. G., Pattison D. R. M. & Zaleski E. 2004. The Hemlo gold deposit, Ontario: An example of melting and mobilization of a precious metal-sulfosalt assemblage during amphibolite facies metamorphism and deformation. *Economic Geology* **99**, 1063–1084.

Tuhumwrire J. T. 1991. *The geology of the Karasuk series (Mozambique belt) in Uganda*. Department of Geological Survey and Mines, Uganda. Report No. JTT/18.

Wayland E. J. 1934. *Crystalline gold and the possibilities of auriferous lodes in the vicinity of the Muti stream, Buhweju-Ankole*. Department of Geological Survey and Mines, Uganda. Bulletin for 1933–38.

Wayland E. J. 1937. *Brief account of some mineral occurrence in Uganda*, Department of Geological Survey and Mines, Uganda.

Westerhof A. B. 2012. *In*: Elepu et al. (2011a) *Summary Report on the Geology and Geodynamic Development of Uganda*, Department of Geological Survey and Mines, Uganda.

Williams C. E. F. 1966. *The geological map of Karamoja area, 1:250,000*, Department of Geological Survey and Mines, Uganda.

Yeats C. J., McNaughton N. J. & Groves D. I. 1996. SHRIMP U–Pb geochronological constraints on Archean volcanic-hosted massive sulphide and lode gold mineralization at Mount Gibson, Yilgarn craton, Western Australia. *Economic Geology* **91**, 1354–1371.

Received 13 July 2013; accepted 14 July 2013